

A Simple Bipolar Jet Model for the Polarization of Core-Collapse Supernovae

David J. Jeffery

Physics Department, University of Nevada, Las Vegas, Box 454002, 4505 Maryland Parkway Las Vegas, Nevada 89154, U.S.A.

jeffery@physics.unlv.edu

ABSTRACT

We propose a bipolar jet model for supernova polarization. Light from the main component of the supernova (which we call the bulk supernova for short) scatters off electrons in the jets and is polarized: this polarized light is added to the direct emission from the bulk supernova and causes the overall supernova emission to be polarized. The motivation for the bipolar jet model is to resolve the potential paradox set by an analysis which suggests strong spherical symmetry for Type Ib supernovae and the expectation that Type Ib supernovae should be highly polarized in the continuum up to perhaps $\sim 4\%$. For the model we have derived simple, non-relativistic, approximate analytic formulae for relative amount of scattered flux and polarization. The polarization formula qualitatively reproduces two main features observed for at least some supernovae: (1) the rise to a polarization maximum and then decline with time; (2) the inverted P Cygni polarization profiles of lines. The model is strictly axisymmetric and predicts a constant position angle of intrinsic polarization. Since position angle variation of intrinsic polarization is observed, the model cannot account for all the polarization of all supernovae.

Subject headings: supernovae: general—polarization—radiative transfer

1. Introduction

1.1. Supernova Polarization in General

Evidence has accumulated that net emission from core-collapse supernovae is often, perhaps usually (or maybe even nearly always), intrinsically polarized. So far the observations show a range in intrinsic continuum polarizations from $\sim 0\%$ up to perhaps 4% with of

order 1 % being typical (e.g., Wang et al. 1996, 2001; Wheeler & Benetti 2000; Leonard et al. 2000a,b; Leonard & Filippenko 2001; Leonard et al. 2001). (The $\sim 4\%$ polarization was actually obtained for a Type Ic supernova [Wang et al. 2001, but we assume it here as a tentative general upper limit on core-collapse supernova continuum polarization.] P Cygni line trough polarization features can exhibit higher polarization than the continuum: at the moment 4 % for Ca II line trough of SN 1987A seems to be the record (Jeffery 1991b, Fig. 16). The apparent polarization trends are that polarization increases with time from explosion for perhaps up to of order 200 days or more and that it increases with decreasing hydrogen/helium envelope mass of progenitor at the time of explosion. The sequence of decreasing hydrogen/helium envelope mass in core-collapse supernova types is II-P, II-L, II-n, IIb, Ib, and Ic (Leonard et al. 2001). The order of II-L, II-n, and IIb is uncertain. For an explanation of the supernova classification scheme see reviews by, e.g., Filippenko (1997), Wheeler & Benetti (2000), and Cappellaro & Turatto (2001). (Type Ia supernovae [thermonuclear supernovae] seem to be usually much less polarized or unpolarized [Wang et al. 1996; Wheeler & Benetti 2000] although some detections have been reported [Wang et al. 1997; Leonard et al. 2000b; Howell 2001]. We will not discuss Type Ia supernovae further in this paper.)

The presence of intrinsic polarization shows some sort of asymmetry exists in the supernova ejecta or the near-supernova environment and that there is some sort polarizing scattering off electrons in the ejecta or, perhaps, dust well away from the actual ejecta. The continuum opacity of supernova atmospheres in the photospheric epoch in the optical and infrared (IR) is in fact dominated by electron scattering opacity (e.g., Wagoner 1981; Harkness 1991), and thus the atmospheres themselves would yield a net polarization if they were asymmetric somehow. Ellipsoidal atmospheres models exploiting electron scattering have been extensively explored (e.g., Shapiro & Sutherland 1982; McCall 1984, 1985; Jeffery 1991a; Höflich 1991; and Howell 2001). Although, electron scattering has virtually no wavelength dependence for photons with energy much less than the electron rest mass energy (e.g., Davisson 1965, p. 51–52), strong line polarization features caused by the combination of electron scattering and line radiative transfer can occur in these models through a mechanism investigated by Jeffery (1989). Another asymmetric supernova model invokes clumps in the ejecta as the cause of asymmetry (e.g., Chugai 1992).

There is a model of supernova polarization that does not require an asymmetric supernova. Instead it invokes a relatively remote scattering from a polarizing dust cloud (Wang & Wheeler 1996). Because the cloud is remote the scattered spectrum is added to the direct supernova spectrum of a later epoch: the scattered spectrum is time-delayed. Dust scattering has a relatively weak polarization wavelength dependence (e.g., Serkowski 1973), but the time-delay effect can give rise to line polarization features due to the variation of

the line profiles over the time delay. (In the bipolar jet model the line polarization features arise through a significant redshift of the jet-scattered flux from its original observer frame wavelength. We call this the redshift effect: see §§ 3.3–3.5 and 4).

A considerable problem in analyzing intrinsic supernova polarization is contamination by interstellar polarization (ISP) caused by intervening dust along the line of sight from the supernova. That intrinsic polarization is present for almost all core-collapse supernovae is proven by the time dependence of the polarization (which would not happen for pure ISP) and the non-ISP wavelength dependence of polarization in particular across lines. (The ISP wavelength dependence is slowly varying and follows the empirical Serkowski law: e.g., Serkowski 1973.) Unfortunately, ISP can completely distort an intrinsic polarization spectrum: e.g., polarization maxima can be turned into minima and vice versa. The correction for ISP must be based on the observed supernova data itself and, alas, on usually somewhat uncertain assumptions. Approaches to ISP correction are discussed by, e.g., Jeffery (1991b), Leonard et al. (2000a), and Wang et al. (2001).

1.2. A Supernova Polarization Paradox and the Bipolar Jet Model

Type Ib supernovae (SNe Ib) lack conspicuous hydrogen lines although most or all may exhibit weak hydrogen Balmer lines (e.g., Branch et al. 2002, hereafter BBK). These supernovae may be essentially helium cores of a few solar masses that result from mass loss by massive stars ($\gtrsim 8 M_{\odot}$ on the main sequence) to a binary companion or in strong winds (e.g., Woosley & Weaver 1994, p. 122ff). The hydrogen remaining may be a few tenths of a solar mass or less which in the supernova ejecta is on the outside moving at velocities $\gtrsim 11,000$ km/s (BBK). (Type Ic supernovae are thought to be similar to SNe Ib, but they have lost even more envelope and show no conspicuous optical helium lines although some helium remains in some cases at least [Filippenko et al. 1995; Clocchiatti et al. 1996]). The rise time to V maximum for low-envelope-mass core-collapse supernovae like SNe Ib is of order 20 days as suggested by earliest observations (e.g., BBK) and theoretically (e.g., Shigeyama et al. 1994; Baron 2001).

Recently, BBK have presented a parameterized LTE analysis of SN Ib spectra. Out of a small, but perhaps representative, sample of 6 SNe Ib BBK find that 5 show photospheric velocity curves (i.e., plots of the photospheric velocity evolution with time) that for the most part vary by $\lesssim 20\%$ from a mean photospheric velocity curve for up to about the first 80 days after explosion. Since photospheric velocity evolution is in fact a function of many properties of a supernova (e.g., mass, density distribution, composition, thermal state), the similar-evolution result strongly suggests that 5 out of 6 supernovae in this sample are quite

alike: tentatively the result suggests that most SNe Ib could be quite alike. Moreover, the members of the subsample of 5 (hereafter the BBK subsample) are probably fairly spherically symmetric or else different viewing orientations would give different photospheric velocity evolutions even if the supernovae were identical.

Recall now that SNe Ib according to the cited trend of increasing polarization with decreasing envelope mass and some observations (McCall 1985; Leonard et al. 2000b) should be highly polarized and have intrinsic continuum polarizations of order 1 % or perhaps sometimes more. To obtain polarization of $\gtrsim 1\%$ from models with ellipsoidal density distributions requires for major-over-minor axis ratios $\gtrsim 1.2\%$ in the iso-density contours (e.g, Höflich 1991; Höflich et al. 2001). Such axis ratios suggest $\gtrsim 20\%$ variations in photospheric velocity curves for identical supernovae seen at the same epoch at different viewing orientations. It seems marginally unlikely that BBK subsample could exhibit the expected polarizations if ellipsoidal asymmetry is assumed.

Unfortunately, only SN 1983N out of the BBK subsample has been measured for polarization. Spectropolarimetry for SN 1983N was briefly reported on by McCall (1985). (The SN 1983N spectropolarimetry data has never been published and now may not be recoverable [McCall (2001)].) A polarization dip from 1.4 % to 0.8 % was found across an Fe II blended line flux emission near 4600 Å near V maximum: the position angle of polarization stayed constant across the emission. The change in polarization across a line profile is a clear signature that intrinsic polarization was present, not just ISP (see § 1.1). The lack of variation in position angle suggests, in fact, that nearly all the polarization was intrinsic and thus that the intrinsic continuum polarization may have been as high as 1.4 %. (Any significant change in the relative amounts of intrinsic polarization and ISP would tend to cause a shift in position angle, unless coincidentally the intrinsic and ISP position angles were aligned.) Thus, at least one of the BBK subsample is significantly polarized and it is the possible they all are.

We face the potential paradox of fairly spherically symmetric supernovae yielding high polarization. To resolve this paradox, we propose a bipolar jet model for the polarization of core-collapse supernovae. In the model, bipolar jets are thrown out of the supernova at the time of explosion. If the jets are thrown out of the supernova core, it is plausible that they are enriched in radioactive ^{56}Ni . The explosion is such that these jets are well collimated and the bulk of the ejecta (which for short we will call the bulk supernova) is left fairly spherical: a contrived picture, but it is what we need for the resolution of the paradox. Since the bulk supernova is fairly spherically symmetric there is no viewing orientation variation in photospheric velocity provided one is not looking nearly down a jet axis. The jets stay sufficiently ionized (perhaps due to radioactive decay of ^{56}Ni and its daughter ^{56}Co) so that

their electron optical depth is high enough that light emitted by the photosphere of the bulk supernova and scattered by the jets into the line of sight is highly polarized. The photosphere and jet are sufficiently remote that the polarization position angle of the scattered light is nearly constant and perpendicular to the plane defined by the jet axis and the line of sight. (See the discussion of the polarization properties of electron scattering in § 3.3.) This means that the polarization of the scattered light is not completely canceled and may amount to a polarization of tens of percent. The polarized scattered light from the jets is only a small contribution to the net supernova flux, but as we will show in § 4 that contribution can give the net flux a significant overall polarization: e.g., $\gtrsim 0.5\%$.

The existence of bipolar jets originating in core-collapse events has been much investigated recently and models have been calculated that show their effects (e.g. Höflich et al. 2001; MacFadyen et al. 2001; Zhang et al. 2003). The jets have been inserted into these models as parameterized entities. It is not clear if they arise naturally in core collapses. Thus, we are free to invoke bipolar jets with the properties we require without justifying them by the results of hydrodynamic calculations.

In § 2 of this paper, we present the structure of our bipolar jet model. Section 3 describes the radiative transfer in the model and derives simple analytic formulae for relative amount of jet-scattered flux (i.e., the relative scattered flux) and the supernova polarization. We assume non-relativistic radiative transfer as a simplifying hypothesis. Because the jet is somewhat remote from the supernova, the scattered spectrum is added to the direct supernova spectrum of a later epoch: thus there is a time-delay effect that also occurred in the dust cloud model of Wang & Wheeler (1996). The time-delay effect could be included in our model, and may sometimes be important even for non-relativistic jets. We also allow for time evolution as the jets expand. Our simplifications allow us to capture the main effects of non-relativistic bipolar jets including time evolution. There are 5 independent basic parameters for the bipolar jet model: θ (or alternatively μ), $\Delta\theta$, τ_{rad} , β_{in} , and b . The τ_{rad} parameter can be reparameterized in terms of physical parameters for the jet (see § 2). In a calculation in which the time-delay effect is included, a reduced time, t_{red} (see § 3.2), replaces τ_{rad} as one of the basic parameters. In a calculation of the time evolution of polarization, the parameter $\tau_{\text{rad},0}t_0^2$ replaces τ_{rad} (see § 2). These parameters are all explained in §§ 2, 3 and 4: see especially § 3.5.

Section 4 reports some demonstration calculations obtained using our analytic formulae. Conclusions and final discussion are given in § 5.

2. The Structure of the Model

We imagine well-collimated, relatively narrow, conical, bipolar jets that emerged from the supernova core during the explosion event. The apex of the cones is at the supernova center, but we picture the jet cones as truncated at the inner and outer ends. The inner and outer ends we assume are sections of spherical shells concentric about the center of the ejecta. This assumption allows us to easily relate jet parameters and jet mass and kinetic energy as we do in this section and gives a simple mental picture for our formulation. In reflection phase of the jets (see § 3.3), we will, in fact, make the contradictory assumption that the inner ends are hemispheres with round sides toward the observer. This may be physically plausible and it permits an analytical treatment. The contradictory assumptions about the inner ends is not a concern. The structure of the real bipolar jets may be complex and we make assumptions that allow us to derive simple analytical formulae that we hope capture the main effect of such jets.

The conical shape of the jets seems physically reasonable for material ejected from the supernova in an axisymmetric fashion as soon as the coasting phase (homologous phase: see below) has set in. We assume the jets are symmetric about the supernova center. The bulk supernova is assumed to be spherically symmetric. The bulk supernova and the jets constitute an axisymmetric system and thus the polarization position angle will be a constant. Given the nature of electron scattering (see § 3.3), this position angle will be perpendicular to the jet axis projected on the sky. (Position angle shifts of 90° are possible in general for axisymmetric systems, but will not occur for the bipolar jet model. See the discussion of the jet polarization in § 3.3.)

The model as just sketched is not, of course, strictly applicable to jets in general. Still one can apply the model to jets in general with the understanding that the parameter values must be treated as characteristic values, not well-defined values. Thus, the model can be applied to observations even if one is not assuming any precise structure for the jets which may for instance be more like clumps or filaments. Simple variations on the model can also be developed for analyzing actual observations.

We consider only the homologous expansion epoch of the ejecta and assume that the jets are participating in the homologous expansion. In homologous expansion, the radial position r_i of any mass element i is given by

$$r_i = v_i t = \beta_i c t , \quad (1)$$

where v_i is the element's constant velocity, β_i is this velocity in units of c , and t is the time since explosion. (At explosion the supernova is usually effectively a point compared the size of the ejecta at observable epochs, and so initial radii are neglected.) Thus in the homologous

expansion epoch, velocity is a good comoving-frame coordinate for the ejecta. In this paper we will usually write velocity in units of c : i.e., we use β 's.

The inner and outer radial velocities of the jets at their inner and outer ends are β_{in} and $\beta_{\text{in}} + \Delta\beta_{\text{rad}}$, respectively: $\Delta\beta_{\text{rad}}$ is the radial velocity length of a jet. The velocities β_{in} and $\Delta\beta_{\text{rad}}$ are time-independent for the homologous expansion epoch, of course. The velocity of the supernova photosphere is β_{ph} : the photosphere is entirely in the bulk supernova. The photospheric velocity is time-dependent since the photosphere recedes into the ejecta as the density and opacity decline with expansion. We assume that $\beta_{\text{in}} \gg \beta_{\text{ph}}$: i.e., the jets are well detached from the bulk supernova. This will allow us to approximate the photosphere as a point source.

The angle of the jet axis from the line-of-sight axis in the direction of the observer is θ . We will often represent this angle by its cosine $\mu = \cos\theta$. We restrict θ to the range $[0, 90^\circ]$, and thus μ to the range $[0, 1]$. The near jet to the observer is at μ and the far jet at $-\mu$.

The half-opening angle of a jet is $\Delta\theta$. The fractional solid angle Ω_{fr} (i.e., solid angle divided by 4π) at the supernova center subtending a jet is given by

$$\Omega_{\text{fr}}(\Delta\theta) = \frac{1}{2}[1 - \cos(\Delta\theta)] \approx \frac{1}{4}\Delta\theta^2 \left(1 - \frac{1}{12}\Delta\theta^2\right) \approx \frac{1}{4}\Delta\theta^2, \quad (2)$$

where the second expression is the 5th order good approximation to the first and the third is the 3rd-order good approximation to the first expression. The 3rd order good expression (used with $\Delta\theta$ in radians) is accurate to better than $\sim 2.3\%$ for $\Delta\theta \leq 30^\circ$ and $\sim 5.3\%$ for $\Delta\theta \leq 45^\circ$.

If we assume that the member of the BBK sample of 6 SNe Ib that did not conform to the mean photospheric velocity curve was non-conforming because the line of sight from the observer to the supernova center passed through a jet, the estimate of the probability of the line of sight passing through a jet is $1/6$. (We have no great confidence in this estimate because of the smallness of the sample and the fact that the bipolar jet model may not be right.) If we assume that all bipolar jet supernovae have the same $\Delta\theta$, then the estimated probability implies that $2\Omega_{\text{fr}}(\Delta\theta) \approx 1/6$ or $\Delta\theta$ of order 35° . (The 2 factor is because our model has two jets.) We will not, however, take 35° as a fiducial half-opening angle $\Delta\theta$: it is not at all a definitive result. The assumptions we will make about the scattering from the jet in § 3 are, in fact, better the smaller $\Delta\theta$.

We will assume we can treat the jets as geometrically narrow since this allows the picture of jet scattering we rely on in § 3.4. For this assumption to be really true

$$\Delta\theta\beta_{\text{in}} \ll \Delta\beta_{\text{rad}} \quad \text{or} \quad \Delta\theta \ll b, \quad (3)$$

where $\Delta\theta$ is in radians, of course, and

$$b \equiv \frac{\Delta\beta_{\text{rad}}}{\beta_{\text{in}}} . \quad (4)$$

The parameters b and β_{in} are chosen as two of the independent basic parameters of the model. The parameter $\Delta\beta_{\text{rad}}$ is a dependent parameter with this choice. We do study the behavior of the relative flux and polarization formulae (see § 3) for $\Delta\theta$ values that are fairly large and cases with $\Delta\theta > b$ in § 4 with the understanding that our assumed pictures of scattering in the jet (see § 3) are becoming poorer and must become invalid at some point as $\Delta\theta$ grows large or b small.

We will neglect occultation effects in our model. Occultation (partial or total) will occur, of course, for θ sufficiently small: i.e., the near jet will occult the supernova photosphere and perhaps the far jet; the supernova photosphere will occult the far jet. Given our assumption that the jets are well detached (i.e., $\beta_{\text{in}} \gg \beta_{\text{ph}}$), occultation should occur only for relatively small θ : in the limit of $\beta_{\text{ph}} \rightarrow 0$, occultation would only occur for $\theta \leq \Delta\theta$. Our expression for polarization will in fact go to zero for θ going to zero which is also what it should do if occultation were considered: the supernova and jets are axisymmetric about the line of sight when $\theta = 0$, and so cannot yield a net polarization whether or not occultation is considered. There may well be distinct effects on the line spectra caused by jet occultation. But those effects and the occultation situation in general are beyond the scope of this paper and we leave them for future consideration *sine die*.

We assume the jets have a spatially constant electron density, density and ionization state. We also assume the ionization state is constant in time which means their electron density falls as t^{-3} due to homologous expansion. The jet electron density is

$$n_e = \frac{\rho}{m_a \mu_e} = \frac{M}{m_a \mu_e \Omega_{\text{fr}}(\Delta\theta) (4\pi/3) [(b+1)^3 - 1] \beta_{\text{in}}^3 c^3 t^3} , \quad (5)$$

where ρ is mass density, $m_a = 1.66053886 \times 10^{-24}$ g is the atomic mass unit, M is the total mass of a jet, and μ_e is the mean atomic mass per electron which is determined from

$$\frac{1}{\mu_e} = \sum_i \frac{X_i Z_i}{A_i} \quad (6)$$

(e.g., Clayton 1983, p. 84): for ion i , X_i is mass fraction, Z_i ionization stage, and A_i atomic mass. Assuming constant ionization state in time implies that μ_e is constant in time too.

The radial optical depth of a jet is

$$\tau_{\text{rad}} = n_e \sigma_e \Delta\beta_{\text{rad}} c t \quad (7)$$

$$\begin{aligned}
&= \frac{3}{4\pi} \frac{\sigma_e}{m_a} \frac{M}{\mu_e \Omega_{\text{fr}}(\Delta\theta)} \frac{b}{[(b+1)^3 - 1]} \frac{1}{\beta_{\text{in}}^2 c^2 t^2} \\
&\approx 2.309 \times \left(\frac{M}{0.1 M_\odot} \right) \left(\frac{4}{\mu_e} \right) \left(\frac{20^\circ}{\Delta\theta} \right)^2 \left[\frac{(2^3 - 1)b}{(b+1)^3 - 1} \right] \\
&\quad \left(\frac{0.06}{\beta_{\text{in}}} \right)^2 \left(\frac{20 \text{ days}}{t} \right)^2,
\end{aligned}$$

where $\sigma_e = 0.665245873 \times 10^{-24} \text{ cm}^2$ is the Thomson cross section for electron scattering and the final expression is in terms of fiducial values with $\Omega_{\text{fr}}(\Delta)$ approximated by $\Delta\theta^2/4$ (which is accurate to better than $\sim 2.3\%$ for $\Delta\theta \leq 30^\circ$ and $\sim 5.3\%$ for $\Delta\theta \leq 45^\circ$ as mentioned above). We emphasize that τ_{rad} decreases monotonically with time and becomes constant (in fact 0) only when time t goes to infinity.

At present there is insufficient guidance for the fiducial values. The total mass ejected by typical SNe Ib is perhaps only $5M_\odot$ or less (e.g., Hachisu et al. 1991), and one might guess the bulk spherical symmetry cannot be maintained unless a jet mass was of order tenths of a solar mass or less: hence we choose $0.1 M_\odot$ as the fiducial jet mass. The ejecta is expected to be helium enriched with intermediate mass elements, and perhaps some hydrogen: we have chosen the fiducial μ_e to be that of singly ionized helium with the helium atomic mass set to 4 exactly: thus the fiducial $\mu_e = 4$. The fiducial $\Delta\theta = 20^\circ \approx 1/3$ radians and $b = 1$ are just a round numbers consistent with $\Delta\theta \ll b$ (with $\Delta\theta$ in radians of course) (i.e., consistent with geometrically narrow jets) that turn out to yield fairly high polarization (see § 4.2). The fiducial time $t = 20$ days was chosen since that is the order of the rise time to V maximum for low-envelope-mass core-collapse supernovae (see § 1.2). The fiducial $\beta_{\text{in}} = 0.06$ (i.e., inner end velocity $\sim 18,000 \text{ km/s}$) is about twice the photospheric velocity at V maximum and about three times the photospheric velocity at 30 days after V maximum according to the mean photospheric velocity curve of the BBK subsample. The choice of 0.06 as the fiducial β_{in} is consistent for V maximum epoch (marginally at least) and for later times with our assumption that $\beta_{\text{in}} \gg \beta_{\text{ph}}$ which allows us to approximate the photosphere as a point source.

We note that with our fiducial values, the jets will have considerable kinetic energy. For one jet, a characteristic kinetic energy is

$$\text{KE}_{\text{char}} \approx \frac{1}{2} M v_{\text{char}}^2 \approx 0.724 \times \left(\frac{M}{0.1 M_\odot} \right) \left[\frac{\beta_{\text{in}}(1 + b/2)}{0.09} \right]^2 \text{ foe}, \quad (8)$$

where $v_{\text{char}} = \beta_{\text{in}}(1 + b/2)c$ is a characteristic velocity, foe stands for 10^{51} ergs (the standard unit of supernova explosion kinetic energies), and we have used the fiducial values for M , β_{in} , and b (see eq. [7] above). Since the whole kinetic energy of an ordinary supernova

is of order 10^{51} ergs (e.g., Woosley & Weaver (1994), p. 90), our fiducial values and v_{char} value require that the jets make large energy demands on the explosion mechanism. We are not concerned about this here. First, our fiducial values and v_{char} value were chosen without much guidance: perhaps less demanding values will turn out to be better in actual polarization spectrum analyses. Second, the actual energy in neutrinos available in core-collapse explosions is of order 10^{53} ergs (e.g., Woosley & Weaver (1994), p. 90). It is thought that some of this available energy is transformed into the kinetic energy of the ejecta and is the main energy of the explosion. But how this is done exactly and how much energy is transformed are still very uncertain (e.g., Janka et al. 2004). Thus, we are plausibly free to invoke jet energies of order 10^{51} ergs for our hypothetical jets. Hydrodynamic jet calculations also somewhat freely invoke jet energies (e.g., Höflich et al. 2001; MacFadyen et al. 2001; Zhang et al. 2003).

For our choice of fiducial values, we obtain jet radial optical depth 2.309 which is sufficient to produce fairly large polarization: see § 4.2. However, as equation (7) shows the optical depth decreases as $1/t^2$. Thus for increasing time with the other parameters fixed the optical depth falls and eventually polarization must decrease because few photons are being scattered and polarized. For example by day 100 (after the explosion) the radial optical is 0.09 from equation (7). Such a low optical depth would usually give very low polarization compared to earlier times. But significant polarization for days 100 to 200 can be obtained from a different choice of parameters for the jets. The plausibility of these choices needs to be investigated.

In an analysis where one does not want to specify the jet mass or mean atomic mass per electron μ_e , one can just specify

$$\tau_{\text{rad}} = \tau_{\text{rad},0} \left(\frac{t_0}{t} \right)^2, \quad (9)$$

where $\tau_{\text{rad},0}$ is a fiducial radial optical depth at a fiducial time t_0 . Actually there is only one parameter $\tau_{\text{rad},0} t_0^2$, but splitting $\tau_{\text{rad},0} t_0^2$ into two factors is an intelligible reparameterization: one might choose $\tau_{\text{rad},0} = 1$ in all cases and then t_0 would become the single parameter. In this paper, we will often just use τ_{rad} itself as a parameter and for time just a reduced time defined by

$$t_{\text{red}} = \frac{1}{\sqrt{\tau_{\text{rad}}}} \quad \text{with the inverse relation being} \quad \tau_{\text{rad}} = \frac{1}{t_{\text{red}}^2}. \quad (10)$$

Note that when $\tau_{\text{rad}} = 1$, $t_{\text{red}} = 1$. The $t_{\text{red}} = 1$ epoch is important for jet polarization. Once the optical depth through a jet falls below ~ 1 , the fraction of direct flux being scattered by the jet must start declining, and thus so must the jet polarization (see § 4.2).

Using equations (7) and (10) we find the relation of time to reduced time to be

$$t = t_{\text{red}} \sqrt{\tau_{\text{rad},0} t_0^2} = t_{\text{red}} \sqrt{\frac{3}{4\pi} \frac{\sigma}{m_a} \frac{M}{\mu_e \Omega_{\text{fr}}(\Delta\theta)} \frac{b}{[(b+1)^3 - 1]} \frac{1}{\beta_{\text{in}} c}} \quad (11)$$

$$\approx 30.39 \text{ days} \times t_{\text{red}} \sqrt{\left(\frac{M}{0.1 M_\odot}\right) \left(\frac{4}{\mu_e}\right) \left[\frac{(2^3 - 1)b}{(b+1)^3 - 1}\right] \left(\frac{20^\circ}{\Delta\theta}\right) \left(\frac{0.06}{\beta_{\text{in}}}\right)}, \quad (12)$$

where the final expression is in terms of our fiducial values for the parameters and we have approximated $\Omega_{\text{fr}}(\Delta)$ by $\Delta\theta^2/4$ again. If the fiducial values are used, we see that $t_{\text{red}} = 1$ and $\tau_{\text{rad}} = 1$ occur at day 30.39 after the explosion.

Another quantity we will need is the radial velocity, which we will call β_{scat} , which locates the place in the jet that is the mean optical depth into the jet that photons radially incident on the jet reach for their first scattering under the assumption that they do scatter in the jet. This mean optical depth τ_{mean} is given by

$$\tau_{\text{mean}} = \begin{cases} 1 - \frac{\tau_{\text{rad}}}{\exp(\tau_{\text{rad}}) - 1} & \text{in general;} \\ 1 & \text{for } \tau_{\text{rad}} \gg 1; \\ \frac{1}{2} \tau_{\text{rad}} \left(1 - \frac{\tau_{\text{rad}}}{6} + \frac{\tau_{\text{rad}}^3}{360}\right) & \text{for } \tau_{\text{rad}} \lesssim 1. \end{cases} \quad (13)$$

At $\tau_{\text{rad}} = 0$, $\tau_{\text{mean}} = 0$; τ_{mean} then grows monotonically with τ_{rad} initially with slope 1/2; but the slope decreases monotonically with τ_{rad} and τ_{mean} goes asymptotically to 1 as $\tau_{\text{rad}} \rightarrow \infty$: $\tau_{\text{mean}}(\tau_{\text{rad}} = 1) \approx 0.418$, $\tau_{\text{mean}}(\tau_{\text{rad}} = 3) \approx 0.843$, and $\tau_{\text{mean}}(\tau_{\text{rad}} = 5) \approx 0.966$. The only stationary point of τ_{mean} is a maximum at $\tau_{\text{rad}} = \infty$. In supernova time evolution, τ_{mean} is nearly a constant 1 at early times when τ_{rad} is large, and then decreases as τ_{rad} decreases; τ_{mean} is decreasing roughly linearly with τ_{rad} when τ_{rad} falls to of order 1; then τ_{mean} vanishes linearly with τ_{rad} as time goes to infinity.

Since the electron density is assumed uniform, β_{scat} is given by

$$\beta_{\text{scat}} = \beta_{\text{in}} + \Delta\beta_{\text{rad}} \frac{\tau_{\text{mean}}}{\tau_{\text{rad}}} = \Delta\beta_{\text{rad}} \left(b^{-1} + \frac{\tau_{\text{mean}}}{\tau_{\text{rad}}}\right) = b\beta_{\text{in}} \left(b^{-1} + \frac{\tau_{\text{mean}}}{\tau_{\text{rad}}}\right). \quad (14)$$

We take β_{scat} to be the characteristic comoving-frame radius for scattering in the jet. At late times when $\tau_{\text{rad}} \rightarrow 0$, $\beta_{\text{scat}} \rightarrow \beta_{\text{in}} + \Delta\beta_{\text{rad}}/2$.

We will also need the optical depth perpendicular to the jet axis from the jet axis to the jet surface at β_{scat} . We call this the off-radial optical depth τ_{off} . The approximate expression for τ_{off} (with $\Delta\theta$ in radians) is

$$\tau_{\text{off}} = \Delta\theta \beta_{\text{scat}} \frac{\tau_{\text{rad}}}{\Delta\beta_{\text{rad}}} = \Delta\theta \left(\frac{\tau_{\text{rad}}}{b} + \tau_{\text{mean}}\right). \quad (15)$$

For high polarization, it is good to have τ_{rad} large for lots of polarizing scattering and τ_{off} small for low depolarizing multiple scattering (see § 3.4). This means $\Delta\theta/b \ll 1$ is a desirable condition for high polarization: we have, in fact, already indicated our need for this condition (which implies a geometrically narrow jet) above (see eq. [3]). In another perspective, τ_{rad} large and τ_{off} small together imply a geometrically narrow jet since we are assuming constant electron density in the jet.

Mathematically, τ_{off} always decreases with decreasing τ_{rad} or increasing time. Its behavior is summarized in the following expressions:

$$\tau_{\text{off}} \approx \Delta\theta \begin{cases} \left(\frac{\tau_{\text{rad}}}{b} + \tau_{\text{mean}} \right) & \text{exactly;} \\ \frac{\tau_{\text{rad}}}{b} & \text{for early times when } \tau_{\text{rad}} \gg 1 \text{ and } \tau_{\text{rad}} \gg b; \\ \frac{\tau_{\text{rad}}}{b} & \text{for all times if } b \ll 2; \\ \tau_{\text{rad}} \left(\frac{1}{b} + \frac{1}{2} \right) & \text{for late times when } \tau_{\text{rad}} \lesssim 1; \\ 1 & \text{for intermediate times if } b \gg 2; \\ & \tau_{\text{rad}}/b \ll 1, \text{ and } \tau_{\text{rad}} \gg 1. \end{cases} \quad (16)$$

Note the following also. If $b < 2$, then $\tau_{\text{rad}}/b > \tau_{\text{mean}}$ always, except at time going to infinity where both τ_{rad} and τ_{mean} are zero. If $b = 2$, then τ_{rad}/b and τ_{mean} asymptotically approach each other as time goes to infinity. If $b > 2$, then there is a phase where $\tau_{\text{rad}}/b < \tau_{\text{mean}}$, that ends only when time goes to infinity.

The time evolution of τ_{rad} and τ_{off} control the time evolution of bipolar jet model polarization as we will see from the analytic polarization formula equation (48) and equation (42) in § 3.5. An interesting prediction of the bipolar jet model emerges from this control is there are two kinds of phases in which the continuum polarization can plateau for some time interval if we assume that no significant time dependence affects the continuum polarization through the redshift effect (see § 3.3). The first kind occurs at early times going back to time zero when τ_{rad} and τ_{off} are both effectively infinite for a finite time: effectively infinite since they enter the function controlling polarization evolution through the functions $1 - \exp(-\tau_{\text{rad}})$ and $\exp(-\tau_{\text{off}})$ (see § 3.5, eq. [42] and [48]) and make those functions nearly exactly 1 and 0, respectively for a finite time. This kind of polarization plateau phase is demonstrated in the calculations in § 4.2: see the early-time, non-infinite b polarization evolution curves in Figures 1, 2, and 3 in § 4.2.

The second kind of polarization plateau phase occurs at intermediate times for $b \gg 2$ or back to time zero for $b = \infty$. In this case, τ_{rad} is effectively infinite in the functions $1 - \exp(-\tau_{\text{rad}})$ and τ_{mean} making both these functions nearly 1 for a finite time, but, on the

other hand, $\tau_{\text{rad}}/b \ll \tau_{\text{mean}} \approx 1$ for a finite time (which situation requires $b \gg 2$) and this makes $\tau_{\text{off}} \approx \Delta\theta$ (with $\Delta\theta$ in radians, of course) for a finite time. In other words, one requires $\tau_{\text{rad}}/b \ll 1$ while $\tau_{\text{rad}} \gg 1$ for the second kind of polarization plateau. The second kind of polarization plateau phase is also demonstrated in § 4.2: see the polarization evolution curves with $b \gtrsim 100$ in Figures 1 and 3.

That the polarization plateau phases can exist is a mathematical prediction of the bipolar jet model. The first kind of plateau phase is unavoidable if our assumptions are adequate and should be observable if a supernova with jets is observed early enough. The second kind can only exist if $b \gg 2$: we show calculations without the second kind of polarization plateau in Figures 2 and 3 in § 4.2. The second kind of polarization plateau is probably physically unrealizable for cases of significant polarization as we discuss in § 4.2.

3. The Radiative Transfer of the Model

In the derivation of the bipolar jet model formulae for scattered flux, relative scattered flux, and polarization, we make many simplifying assumptions. These assumptions are needed to capture the main effect of the model on flux and polarization analytically and tractably. One main simplifying assumption is that the only significant opacity in a jet is electron scattering (or Thomson) opacity. Thus we neglect the scattering, absorbing, and depolarizing effects of other opacities of which line opacity is probably the most important. Another consequence of assuming only electron scattering opacity is that no photons are destroyed in the jet. We also assume none are created.

In § 3.1, we will make the point source assumption for the spherically symmetric bulk supernova. Subsection 3.2, gives a simplified treatment of the time-delay effect which could be incorporated into the bipolar jet model. In the following three subsections, we derive analytic formulae for scattered flux, scattered relative flux, and polarization spectra that account for the three phases of jet polarization. The first phase, which we call the reflection phase, is when the jet is optically thick in all directions (see § 3.3). The second phase, which we call the radial phase, is when jet is optically thick in the radial direction, but optically thin in the direction perpendicular to the jet axis (see 3.4). The third phase, which we call the optically-thin phase, is when the jet is optically thin in all directions (see § 3.4). In § 3.5, we give general expressions that are for all phases.

3.1. The Point Source Approximation for the Supernova

Given that the direct luminosity from the supernova (i.e., the luminosity without the jet contribution) at rest-frame wavelength λ is $L_{\text{dir}}(\lambda)$, the direct flux at Earth from the supernova (i.e., the flux without the jet contribution) is

$$f_{\text{dir}}(\lambda) = \frac{L_{\text{dir}}(\lambda)}{4\pi D^2}, \quad (17)$$

where D is the Earth-supernova-center distance.

The fraction of $L_{\text{dir}}(\lambda)$ that enters the inner end of a jet is just $\Omega_{\text{fr}}(\Delta\theta)$ (see eq. [2] in § 2). This is true regardless of the size of the supernova photosphere (provided $\beta_{\text{ph}} \leq \beta_{\text{in}}$): it is a consequence of the assumed spherical symmetry of the spherical bulk of the supernova. We will assume that $L_{\text{dir}}(\lambda)\Omega_{\text{fr}}(\Delta\theta)$ is all the luminosity that passes through a jet and that all the beams from the bulk supernova are radial: i.e., all the beams from the bulk supernova that enter a jet are radial and they enter at the inner end and they leave at the outer end. Thus we are making the point-source approximation for the photosphere. This approximation should be reasonably good as long as $\beta_{\text{in}} \gg \beta_{\text{ph}}$ as we have already assumed (see § 2). There are, of course, two errors associated with the approximation caused by non-radial beams from a finite photosphere. First, there will be non-radial beams entering the inner end of a jet (these are counted in $L_{\text{dir}}(\lambda)\Omega_{\text{fr}}(\Delta\theta)$, of course) and these beams will not always traverse the whole radial extent of the jet. Second, there will be non-radial beams that enter the sides of a jet (these are not counted in $L_{\text{dir}}(\lambda)\Omega_{\text{fr}}(\Delta\theta)$, of course) and these beams will only traverse some part of the radial extent of the jet. The first error leads to an overestimate of and the second error, to an underestimate of the direct-flux-jet interaction when we make the point-source approximation. The two errors are somewhat compensating: this somewhat strengthens point-source approximation. The point-source approximation is also somewhat strengthened by the fact that the photospheric emission will be somewhat limb-darkened: thus the photosphere will be more point-like than assuming that angle-independent specific intensity beams emerge from it. Thus, our photosphere is more point-like than a non-zero β_{ph} suggests at first.

3.2. The Time-Delay Effect

The time-delay effect is caused by the supernova evolving during the time that flux travels from the photosphere to the jets and during the radiative transfer through the jets. In this section we will develop some formalism to treat the time-delay effect in the bipolar jet model, but we will not actually incorporate this formalism into our formulae in §§ 3.3,

3.4, and 3.5 and our calculations in § 4. The variations on those formulae that allow for the time-delay effect can easily be derived if needed, but are a bit cumbersome in appearance.

In general, time-delay effect will be complex. So we will make some simplifying assumptions. We will assume again that the bulk supernova can be treated as a point at the center of the system and we will assume that the jet can be treated as a point at velocity β_{scat} (see § 2, eq. [14]) for time-delay effect purposes: this eliminates the need to consider the time delays while flux transfers through the jets. Now β_{scat} itself is time dependent. As a simplification we assume it can be evaluated at a fiducial time t : t and all other times below are counted from the time of the supernova explosion: i.e., since time zero. This last assumption is actually rather poor since the time-delay effect will cause us to evaluate jet optical depth parameters at times different than t (as we will see below) and those optical depth parameters determine β_{scat} . But to get a sense of the time-delay effect, it is adequate.

For each time of observation of flux and polarization spectra, we will in general have to consider 5 supernova evolution times. But we will compact the expressions by using an upper case label for the near jet and a lower case label for the far jet. Let $t_{\text{jet}\pm}$ be the time that flux arrives at a jet from the bulk supernova. Let $t'_{\text{jet}\pm}$ be the time that same flux started out from the bulk supernova. The direct flux from the bulk supernova that starts at fiducial time t arrives at the Earth at the same time as the flux from the jet that starts at time $t_{\text{jet}\pm}$: as mentioned above, we assume no time delay for the flux inside the jet. From geometry and homologous expansion, it follows that

$$t_{\text{jet}\pm} = t'_{\text{jet}\pm} + \frac{\beta_{\text{scat}} c t_{\text{jet}\pm}}{c} \quad \text{and} \quad t_{\text{jet}\pm} = t \pm \frac{\mu \beta_{\text{scat}} c t_{\text{jet}\pm}}{c}, \quad (18)$$

where μ (as specified in § 2) is the cosine of the angle to the near jet: we confine μ to the range $[0, 1]$. A little algebra leads to

$$t'_{\text{jet}\pm} = t \frac{1 - \beta_{\text{scat}}}{1 \mp \mu \beta_{\text{scat}}} \quad \text{and} \quad t_{\text{jet}\pm} = t \frac{1}{1 \mp \mu \beta_{\text{scat}}}. \quad (19)$$

From the expressions of equations (18) and (19), we have at once the inequalities

$$t'_{\text{jet}+} \leq t \leq t_{\text{jet}+} \quad \text{and} \quad t'_{\text{jet}-} \leq t_{\text{jet}-} \leq t. \quad (20)$$

The inequalities show the time ordering of the events. Note that $t_{\text{jet}\pm} = t$ only when $\mu \beta_{\text{scat}} = 0$ and $t'_{\text{jet}\pm} = t_{\text{jet}\pm}$ only when $\beta_{\text{scat}} = 0$. Note also that the ratios of the time parameters are not constant since β_{scat} is itself time dependent. We have recall simplified this time dependence by assuming that we can evaluate β_{scat} at the fiducial time t itself.

Equation (19) is the probably the most useful time-delay effect result since fiducial time t is the natural time for any calculation: it is the time that characterizes the bulk of the

flux that ones sees: sees D/c later than t , of course: recall D is the Earth-supernova-center distance.

As we will see in §§ 3.3, 3.4, and 3.5, polarization is high for $\mu \approx 0$. For example, for a high polarizing jet one might have $\mu = 0$ and $\beta_{\text{scat}} = 0.1$: this implies $t'_{\text{jet}\pm} = 0.9t$. Thus, with these parameters the observer detects a mixture of direct flux and scattered flux where the scattered flux originated in the bulk supernova at at time 10 % earlier than the time of origin of the direct flux. Since considerable evolution in flux level and spectra can occur in 10 % of the time since explosion, the time-delay effect could be significant. Thus, in general it would be useful to have a complete enough time coverage of observed flux spectra so that one can use the observed spectra from earlier times to construct synthetic polarization spectra using the bipolar jet model for later times.

Equation (19) can be used with reduced times (see § 2) replacing ordinary times: i.e., t becomes t_{red} , $t_{\text{jet}\pm}$ becomes $t_{\text{red jet}\pm}$, and $t'_{\text{jet}\pm}$ becomes $t'_{\text{red jet}\pm}$. Using t_{red} as the fiducial time and equation (19), and equations (10), (13), and (15) of § 2, one can calculate the needed time-delay affected optical depths for t_{red} . Also using t_{red} and equation (19), one can calculate the times at which the flux from the jets started out from the supernova (i.e., $t'_{\text{red jet}\pm}$), and thus when calculating the net flux one can add the direct and jet fluxes corrected for the time delay effect. In fact, t_{red} (which replaces t) can be used as of the 5 independent basic parameters of the bipolar jet model when the time-delay effect is included. If one neglects the time-delay effect, τ_{rad} is the same for both jets in a calculation and τ_{rad} can be used instead of t_{red} as one of the 5 independent basic parameters.

We will not explore the consequences of the time-delay effect in detail in this paper. But we will briefly discuss them here. As a heuristic formula (suggested by eq. [48] in § 3.5), let polarization as a function of t be given for the nonce by

$$P(t) \sim P_0(t)\Pi(t) , \quad (21)$$

where $P_0(t)$ is polarization in the absence of time delay and

$$\Pi(t) = \frac{f_{\text{dir}}(\bar{t}'_{\text{jet}})}{f_{\text{dir}}(t)} , \quad (22)$$

where f_{dir} is the direct flux from the bulk supernova and \bar{t}'_{jet} is some appropriate average of $t'_{\text{jet}+}$ and $t'_{\text{jet}-}$. As shown by the demonstration results in § 4, there will be a time of maximum (continuum) polarization. These demonstration calculations were done neglecting the time-delay effect, and so their polarization corresponds to what we have labeled for the nonce $P_0(t)$. Clearly, if $\Pi(t)$ is a rising/falling function at the time of the $P_0(t)$ maximum (which is a stationary point recall), then the $P(t)$ maximum will be shifted to a later/earlier time than that of $P_0(t)$ maximum.

Now it is difficult to predict the temporal behavior of $\Pi(t)$ in general since it depends on the shape of the supernova light curve and on the how \bar{t}'_{jet} varies with time. But near maximum light, $\Pi(t)$ should be a rising function since the $f_{\text{dir}}(\bar{t}'_{\text{jet}})$ will be rising and $f_{\text{dir}}(t)$ should be nearly stationary. So if the $P_0(t)$ maximum is at about maximum light, the time-delay effect will tend to give the $P(t)$ maximum at a later time.

At late times (i.e., probably of order 100 days or more after explosion), β_{scat} will approach a constant $\Delta\beta_{\text{rad}}(b^{-1} + 1/2)$ as $\tau_{\text{rad}} \rightarrow 0$ (see eq. [13] and [14] in § 2), and thus the ratio \bar{t}'_{jet}/t will approach a constant too (see eq. [19]): a constant that is less than 1, of course (see eq. [20]). At such times the light curve of the supernova is falling exponentially or quasi-exponentially (e.g., Jeffery 1999), and so $\Pi(t) \approx \exp[(1 - \bar{t}'_{\text{jet}}/t)t/t_e]$ which is growing exponentially: t_e is the assumed e -folding time of the light curve and the ratio \bar{t}'_{jet}/t is a constant less than or equal to 1 (see eq. [19] and [20]). Thus if the $P_0(t)$ maximum occurs in this late phase, the $P(t)$ maximum will tend to occur at a later time again. Actually, because ejecta is tending to be optically thin in the exponential/quasi-exponential phase, one does not expect the $P_0(t)$ maximum to occur then.

In the analytic formulae we derive in the remainder of this section and in the calculations reported in § 4, we will, as mentioned above, neglect the time-delay effect. This means we approximate all the time parameters by one value, t or t_{red} . When only one time parameter is needed then, as mentioned above, τ_{rad} can be used instead of t_{red} as one of the 5 independent basic parameters.

3.3. Reflection Phase

In the reflection phase, the jet is optically thick and it acts as a diffuse reflector of incident light. Recall that for simplicity we have assumed that the jets have uniform electron density. In fact they are likely to increase in electron density as one moves inward. Thus photons striking the optically thick jet that penetrate somewhat deeply in optical depth will scatter a few times and then tend to diffuse outward again and be emitted from the jet. The behavior of these deep-penetration photons is effectively uninfluenced by their history prior to entering the jet. The deep-penetration photons will have an emergent angular distribution that is rather isotropic over solid angle 2π (i.e., the half of the sky not filled by the jet) and is mostly unpolarized—individual photons will be polarized, but their net flux mostly not. Some anisotropy and net flux polarization will occur due to diffusive photon scattering in an inhomogeneous medium (e.g., Chandrasekhar [1960, p. 248] for plane-parallel atmospheres; Cassinelli & Hummer [1971] for spherically symmetric atmospheres), but this is likely to be a relatively minor effect and too complicated for us to contemplate in the simple picture we are

developing. There is also a class of photons that scatter more than once, but not sufficiently to lose all trace of their history before they entered the jet. Their angular distribution and polarization state are still somewhat determined by their initial direction of incidence on jet: but this non-random redistribution and polarization is likely to have a relatively small effect. We will assume that photons that scatter more than once in the jet emerge unpolarized and are isotropically distributed over 2π .

The photons that scatter once and escape the jet will have an angular distribution and polarization determined by the Rayleigh phase matrix (e.g., see Chandrasekhar 1960, p. 37). We will estimate the fraction q of photons in this category in the following way. The probability that a photon penetrates a jet along some typical beam path to optical depth τ without scattering and then scatters in optical depth $d\tau$ is $\exp(-\tau) d\tau$. Since we are considering a very optically thick phase, we can regard the local jet surface as a plane-parallel atmosphere. Thus $\sim 1/2$ the scattered photons are aimed at a path toward the “plane-parallel” surface and $\sim 1/2$ are directed inward and must scatter more than one time before escaping: we assume these fractions are both exactly $1/2$. This half-inward-half-outward division among scattered photons is true even with the anisotropic Rayleigh distribution since this distribution is axisymmetric about the incident direction and forward-back symmetric: any plane through a polar plot of the distribution slices it into two regions with the same integrated emission. We will assume that the average optical depth distance to escape the jet for a photon that has just scattered for the first time is equal to τ : note the penetrating and escaping directions are not the same; we are just assuming the optical depth along them is the same in some kind of average sense. Thus the probability of this photon escaping without scattering again is estimated to be $\exp(-\tau)$. If we multiply the relevant factors together, we find the estimate of the probability of a photon incident on the jet penetrating to optical depth region $d\tau$ and then escaping the jet is $(1/2) \exp(-2\tau) d\tau$. The estimated q fraction is the integral of $(1/2) \exp(-2\tau) d\tau$ over all τ :

$$q \approx \frac{1}{2} \int_0^\infty \exp(-2\tau) d\tau = \frac{1}{4} , \quad (23)$$

where the integral can be extended to infinite optical depth because we are assuming the jet is optically thick. If one had a well specified jet structure, one could calculate more exactly the average fraction of once-scattered photons. That calculation is too elaborate for our crude picture of the jet. In this paper, we adopt $1/4$ as the fixed value for q .

To treat polarization we must label polarization axes for the scattered light. We will label these axes (which are both perpendicular to the scattered light’s propagation direction) x and y : the x axis is perpendicular to the plane of scattering and the y axis is aligned with it. The plane of scattering (or scattering plane) is the plane defined by incident and scattered

beams. The Stokes Q and U parameters are needed to evaluate the polarization: see Chandrasekhar (1960, p. 25) for a detailed presentation of the Stokes parameters. The Stokes Q parameter for the scattered flux in our setup is y -flux minus the x -flux following conventions of Chandrasekhar (see Chandrasekhar 1960, p. 27).

Because of the finite size of the jet there will be a range of scattering planes for light scattered in the observer direction. In our mental picture, we will approximate this range of planes by the plane defined by the jet axis and the scattering direction to the observer: we will call this plane the fiducial plane. Just using the fiducial plane alone would overestimate the polarizing effect since the polarization-canceling effect from a range of planes is neglected. We will make a crude correction factor for the Stokes Q formula to account for the range of scattering planes.

Consider a circular arc of material in the jet with arc center at the center of the supernova in the plane defined by the jet axis and the line perpendicular to the line of sight. The arc is meant to approximate the layer of scattering material in the jet at β_{scat} . The angle at the jet center subtended by the arc is naturally $2\Delta\theta$. Measure the angle for any point along the arc by ζ : $\zeta = 0$ at the jet axis and is positive counterclockwise. Suppose again that the supernova photosphere is a point. Emission from the supernova center is scattered off electrons in the arc toward the observer. Assume the incident specific intensity on the arc, the amount of scattering, and the polarizing effect are constant along the arc. The local Stokes axes at each point along the arc are labeled x' (tangent to the arc) and y' (perpendicular to the arc). The unadorned x and y axis are fiducial axes for the fiducial plane. The local Stokes parameters are dQ' and dU' : $dQ' < 0$ from the Rayleigh phase matrix (e.g., see Chandrasekhar 1960, p. 37) and $dU' = 0$ by symmetry: we are assuming the incident light is unpolarized. The local position angle of polarization is aligned with the x' axis: see the Rayleigh phase function (eq. [28]) and accompanying discussion below. If we could legitimately just integrate up the local dQ' without transforming to the fiducial x - y axes, then the net Q' for the arc emission would be proportional to $2\Delta\theta$. More correctly we should transform dQ' and dU' to the fiducial x - y axes and then integrate. The transformations for a rotation ζ clockwise are

$$dQ = dQ' \cos(2\zeta) \quad \text{and} \quad dU = -dQ' \sin(2\zeta) \quad (24)$$

(Chandrasekhar 1960, p. 34).

The integration for net U gives zero because the integration interval is even: from a more obvious perspective, the axisymmetry of the jet requires the net U for the fiducial plane Stokes axes to be zero. Because $U = 0$, the position angle of polarization is determined only by the net Q . Given the nature of electron scattering (which we discuss below), the polarization is aligned perpendicular to the fiducial plane.

The net Q corrected for the variation of the polarization axes along the arc in terms of the net Q' neglecting this variation is given by

$$Q = Q' \frac{1}{2\Delta\theta} \int_{-\Delta\theta}^{\Delta\theta} \cos(2\zeta) d\zeta = Q' \frac{1}{\Delta\theta} \int_0^{\Delta\theta} = Q' \frac{\sin(2\Delta\theta)}{2\Delta\theta} . \quad (25)$$

Thus to crudely correct the Stokes Q parameter in our formulae developed assuming only fiducial plane scattering, we will multiply it by the correction factor

$$\xi(\Delta\theta) = \frac{\sin(2\Delta\theta)}{2\Delta\theta} \approx 1 - \frac{1}{6}(2\Delta\theta)^2 + \frac{1}{120}(2\Delta\theta)^4 , \quad (26)$$

where the second expression is the 5th order good approximation in small $2\Delta\theta$ (in radians) to the first. Since the 1st order term in the correction factor vanishes, we would have 1st order good expression for Q without using the correction factor. The correction factor is, of course, only a crude correction since the jet is not a single arc at a single inclination to the line of sight. But the $\xi(\Delta\theta)$ factor does crudely have the right effect and the exactly right limiting behavior. In the vanishingly-narrow-jet limit $\Delta\theta \rightarrow 0$ and $\xi(\Delta\theta) \rightarrow 1$ as it should since there is no range of scattering planes in this case. In the limit where the jets cover the sky spherically symmetrically $\Delta\theta \rightarrow \pi/2$ and $\xi(\Delta\theta) \rightarrow 0$: this is also correct since the symmetry would cancel all polarization. Between the limits, $\xi(\Delta\theta)$ decreases monotonically with $\Delta\theta$ with the only stationary point being a maximum at $\Delta\theta = 0$. At worst, $\xi(\Delta\theta)$ is an adequate interpolation formula for a correction factor; it should be somewhat better than that though.

A similar Stokes Q parameter correction factor could perhaps be devised to account for the finite size of the supernova photosphere. But it would complicate our mental picture and, given the crudity of the model, seems of little value.

The angular redistribution function for electron scattering of unpolarized light is the normalized Rayleigh phase function:

$$g_{\text{norm}}(\mu_{\text{gen}}) = \frac{1}{4\pi} g(\mu_{\text{gen}}) : \quad (27)$$

$g(\mu_{\text{gen}})$ is the (conventional) Rayleigh phase function given by

$$g(\mu_{\text{gen}}) = \frac{3}{4} (1 + \mu_{\text{gen}}^2) , \quad (28)$$

where μ_{gen} is the cosine of a general scattering angle (i.e., the angle between incident and scattered beam directions) (e.g., Chandrasekhar 1960, p. 35). The net direct supernova light incident on the jets is unpolarized. Individual beams are polarized since the supernova atmosphere is electron-scattering dominated, but spherical symmetry of the bulk supernova

makes the net polarization zero. In our notation the 1 in the $1 + \mu_{\text{gen}}^2$ factor determines the intensity perpendicular to the scattering plane (i.e., the x -flux) and the μ_{gen}^2 , the intensity parallel to the scattering plane (i.e., the y -flux): this follows from the Rayleigh phase matrix (e.g., Chandrasekhar 1960, p. 37). Note that forward and backward scattering are unpolarized since $\mu_{\text{gen}}^2 = 1$ in those cases and the two scattered flux components are equal. Scattering through 90° gives the maximum polarization of 100 %.

The Rayleigh phase function is adequate to describe photon redistribution for us for two reasons. First, we can assume electron scattering is coherent (i.e., does not change wavelength) in the jet frame. The coherent scattering approximation is adequate since the wavelength part of the photon redistribution (which affects the angular redistribution in general) on electron scattering for electrons obeying a Maxwellian distribution (Mihalas 1978, p. 420) averages away for continuum radiative transfer which is all we are considering in the jet. Second, the flux in the jet can be approximated as unpolarized in an average sense before a last scattering which may or may not be polarizing. For the reflection phase considered in this section the last scattering in the jet is only polarizing on average if it is also the first scattering as we argued above. For the radial and optically-thin phases of the jet (see § 3.4), the photons that are only scattering radially inward and outward (i.e., radially directed photons) are approximately unpolarized since their scattering is approximately backward and forward scattering. The last scattering is polarizing if it is of radially-directed, and so unpolarized, photon. If the last scattering of non-radially-directed photon is not polarizing on average as we will argue in § 3.4.

We assume here and in all our developments that all scattering toward the Earth that is polarized (on average) can be treated as being from the jet axis to the direction toward the observer, and so the only cosines of scattering angles for this flux are μ and $-\mu$: i.e., the cosines for the near and far jets from the line of sight in the direction to the observer (see § 2). (For the reflection phase this approximation is justified by our assumption of $\Delta\theta$ small. We justify it for the radial and optically-thin phases in § 3.4.) The approximation is, of course, somewhat gross. The unpolarized (on average) scattered flux toward the observer we approximate as coming from an isotropic angular distribution, and so the cosine of the scattering angle is unneeded and unspecified.

Although we treat the electron scattering as coherent in the jet frame, the supernova flux that scatters off the jet and is emitted toward the observer at rest-frame wavelength λ is redshifted from the rest-frame wavelength λ' that it had on emission from the supernova photosphere. We call this shifting the redshift effect. It is caused by macroscopic-velocity-field Doppler shifts. The approximate relation between the two wavelengths from the non-

relativistic Doppler formula is

$$\lambda = \lambda'_{\pm} [1 + \beta_{\text{scat}} (1 \mp \mu)] , \quad (29)$$

where the upper and lower cases are for scattering off the near and far jets, respectively, from the observer: recall μ is the cosine of the angle of axis of the jets measured from the line of sight axis in the direction of the observer. The β_{scat} velocity was defined in § 2 (see eq. [14]) as the characteristic radial velocity of jet scattering: for the reflection phase $\beta_{\text{scat}} \approx \beta_{\text{in}}$ since the jet is very optically thick, and so $\tau_{\text{mean}}/\tau_{\text{rad}} \ll 1$. There actually will be somewhat more redshift than given by equation (29) caused by multiple scattering in the homologously expanding medium of jet. In the reflection phase those scatterings are close together in velocity space, and so probably cause negligible extra Doppler shift; in later phases such shifts may be significant, but we will neglect them for simplicity. We actually will use the approximate inverse of equation (29) in our formalism below:

$$\lambda'_{\pm} = \lambda [1 - \beta_{\text{scat}} (1 \mp \mu)] , \quad (30)$$

which is an inverse formula good to 1st order in β_{scat} .

To calculate the net jet-scattered flux and the net Stokes Q parameter for this flux in the reflection phase we will, as mentioned at the beginning of § 2, assume the inner ends of the jets as hemispheres with round sides toward the center of the supernova. This assumption may be physically plausible and it allows an analytical treatment. But it does contradict our basic picture of the jet ends as discussed at the beginning of § 2.

Let the cross sectional area of the hemispheres be A . Toward the observer the reflecting face of the near jet hemisphere will be crescent-shaped and that of the far jet hemisphere will be gibbous. The faces of the hemispheres on sky have projected areas

$$\frac{1}{2}(1 \mp \mu)A , \quad (31)$$

where the upper and lower cases are for the near and far jets, respectively. Note that the summed projected area of the jets is just A .

Approximating the supernova photosphere as a distant point source, the hemispheres are wholly illuminated by the direct supernova flux. The direct supernova luminosity (emitted at wavelength λ'_{\pm}) absorbed per unit projected area (i.e., projected area as seen from the supernova center) by a jet is

$$\frac{L_{\text{dir}}(\lambda'_{\pm})\Omega_{\text{fr}}(\Delta\theta)}{A} . \quad (32)$$

An approximate expression for the reflected specific intensity emitted by a hemisphere in the direction toward the observer is

$$\frac{L_{\text{dir}}(\lambda'_{\pm})\Omega_{\text{fr}}(\Delta\theta)}{2\pi A} [g(\mu)q + (1 - q)] . \quad (33)$$

where the $g(\mu)q$ term accounts for the once-scattered, polarized photons, and the $(1 - q)$ for the multiply scattered, unpolarized photons. Recall we assumed that we can approximate all cosines of scattering angles for the once-scattered photons by the μ and $-\mu$. We only need the μ in equation (33) for both jets since the phase factor formula only depends on the square of the scattering angle cosine (see eq. [28]). The denominator $2\pi A$ in equation (33) follows from the following considerations. If the energy absorbed by one jet from the direct flux from the bulk supernova were emitted by specific intensity beams that were constant with angle of emission and surface location from a sphere of radius r , then the denominator would be $4\pi^2 r^2$, where the second π factor accounts for the difference between flux (using in the term in its formal radiative transfer sense) and specific intensity. In our case, all the absorbed direct flux energy gets radiated out of a hemisphere and not a sphere, and so the numerator is set to $2\pi^2 r^2$ or $2\pi A$ taking r to be the radius of the hemisphere.

Equation (33) is approximate because we have assumed a remote point photosphere and because of the approximate nature of the q factor. It is also approximate because we assume that the energy collected from the bulk supernova is spread evenly over the hemispherical surface. Actually the edges of the surface get less energy per surface area than the center because of the hemispherical curvature: the reflection specific intensity should decrease as one moves from center to edges. However, the overall reflected flux works out nearly correctly as we show below probably because of the compensation we get when summing up all the flux from both jet hemispheres emitted toward the observer.

Now the flux at Earth from an object emitting specific intensity I is $f = \int I d\Omega = \int I dA/D^2$, where $d\Omega$ is the differential bit of solid angle at Earth that the object subtends and dA is a differential bit of the projected area of the object on the sky (e.g., Mihalas, p. 11). Given this fact and making use of equations (17), (30), (31), and (33), it follows that the total jet flux measured at Earth at the rest-frame wavelength λ for the reflection phase is

$$f_{\text{reflection}}(\lambda) = \left[f_{\text{dir}}(\lambda'_+)(1 - \mu) + f_{\text{dir}}(\lambda'_-)(1 + \mu) \right] \Omega_{\text{fr}}(\Delta\theta) / [g(\mu)q + (1 - q)] . \quad (34)$$

We note that if λ'_+ and λ'_- are both set to λ and q to zero, then

$$f_{\text{reflection}}(\lambda) = 2 \frac{L_{\text{dir}}(\lambda) \Omega_{\text{fr}}(\Delta\theta)}{4\pi D^2} . \quad (35)$$

This last result is the flux at the Earth if all the luminosity captured by the jets were radiated isotropically. That we get this result verifies that we are accounting for the energy approximately correctly in equation (33) for the reflected specific intensity.

From equation (34) and making use of our understanding of equation (28) for the Rayleigh phase function, we find that the net Stokes Q parameter for the reflected flux is

$$Q_{\text{reflection}}(\lambda) = [f_{\text{dir}}(\lambda'_+)(1 - \mu) + f_{\text{dir}}(\lambda'_-)(1 + \mu)] \Omega_{\text{fr}}(\Delta\theta) \left(\frac{3}{4}\right) (\mu^2 - 1) q \xi(\Delta\theta), \quad (36)$$

where we have introduced the correction factor $\xi(\Delta\theta)$ (see eq. [26]) that accounts for effect of the range of scattering planes on the Stokes Q parameter. Note the $(1 - q)$ term in equation (34) accounts for unpolarized flux, and thus the x - and y -fluxes it governs are equal and it cancels out of $Q_{\text{reflection}}$.

3.4. Radial and Optically Thin Phases

In the ideal picture of the radial phase, a jet is optically thick in the radial direction, and so no photons can escape out the outer end of the jet. On the other hand, we assume the jet is optically thin perpendicular to its axis. With this setup, radially-outward scattered photons remain trapped in the jet as do the radially-inward scattered ones (except at inner end of the jet) and off-radially scattered photons are assumed to escape without scattering again. Recall that forward and backward scattering are unpolarizing as determined by the Rayleigh phase matrix (see § 3.3), and thus the radially scattered photons remain unpolarized. As mentioned in § 3.3, we assume that all scattering toward the Earth can be treated as happening along the jet axis, and so the cosines of scattering angles are again μ and $-\mu$. Thus there is no averaging over a range of scattering cosines. We again will include our correction factor $\xi(\Delta\theta)$ (see § 3.3, eq. [26]) to account for the range of scattering planes. Recall the scattering plane defined by the jet axis and the line of sight to the observer is the fiducial plane.

Given aforesaid picture, all the photons that escape the jet are distributed in angle and polarized as if they had undergone a single electron scattering event (i.e., their last scattering which was off-radial or radially-inward)—except that in our picture there is no flux scattered radially-outward and perhaps less scattered radially-inward since some photons should random walk far out in the radial direction. The exception tends to cause more polarized emission than predicted by the Rayleigh phase matrix for a single scattering. Trying to invent a correction factor for this effect that is of the right size seems futile given the crudity of the model.

To handle the phase where the jet becomes optically thin radially (i.e., the optically-thin phase), we include the factor $1 - \exp(-\tau_{\text{rad}})$ in our expressions for flux and Stokes Q

parameter: $1 - \exp(-\tau_{\text{rad}})$ is the fraction of photons that scatter in the jet at least once: it goes to zero as τ_{rad} goes to zero. Thus the expressions we develop in this section will handle both the radial phase and optically-thin phase.

The ideal picture for radial phase is very polarizing for the direct supernova flux that passes into the jet because of the off-radial direction is optically thin. To make the expressions a bit more realistic we will account for finite optical depth perpendicular to the axis in the following way. As defined by equation (14) in § 2, β_{scat} is the mean velocity position that photons incident on a jet reach for their first scattering. The perpendicular-to-axis optical depth from axis to jet surface at β_{scat} is τ_{off} which is approximately given by equation (15) in § 2. We take $\exp(-\tau_{\text{off}})$ as the characteristic probability that an off-radially scattered photon escapes without scattering again. We take $1 - \exp(-\tau_{\text{off}})$ as the probability that an off-radially scattered photon scatters again. We assume that photons that scatter multiple times in non-radial directions have on average an isotropic angular distribution and zero polarization: the multiple off-radial scattering should average away anisotropy and net polarization.

Now recall that the direct supernova luminosity (emitted at wavelength λ'_{\pm}) passing into a jet is $L_{\text{dir}}(\lambda'_{\pm})\Omega(\Delta\theta)$. Multiplying this by $1 - \exp(-\tau_{\text{rad}})$ gives the luminosity that interacts in the jet: i.e., $L_{\text{dir}}(\lambda_{\pm})\Omega(\Delta\theta)[1 - \exp(-\tau_{\text{rad}})]$. We now assume that all this interacting luminosity escapes with a normalized angular distribution determined by

$$\frac{g(\mu_{\text{gen}}) \exp(-\tau_{\text{off}}) + [1 - \exp(-\tau_{\text{off}})]}{4\pi} \quad ; \quad (37)$$

i.e., a combination of Rayleigh and isotropic scattering with the relative amount of each determined by the probability of no second off-radial scattering $\exp(-\tau_{\text{off}})$. Thus the luminosity per solid angle in the direction of the Earth from a jet at wavelength λ is

$$L_{\text{dir}}(\lambda'_{\pm})\Omega(\Delta\theta)[1 - \exp(-\tau_{\text{rad}})] \frac{1}{4\pi} \{g(\mu) \exp(-\tau_{\text{off}}) + [1 - \exp(-\tau_{\text{off}})]\} \quad , \quad (38)$$

where again the upper case of λ'_{\pm} is for the near jet and the lower case for the far jet, λ'_{\pm} is determined by equation (30) (see § 3.3), and $g(\mu)$ applies to both near and far jets since this formula depends only on the square of the scattering angle cosine (see eq. [28] in § 3.3). If we multiply the luminosity per unit solid angle by $d\Omega_{\text{Earth}}/(D^2 d\Omega_{\text{Earth}})$, where $d\Omega_{\text{Earth}}$ is a differential bit of solid angle at a jet subtended by the Earth and $D^2 d\Omega_{\text{Earth}}$ is the projected area of the Earth on the sky as seen from the jet, we get the flux at Earth from one jet: i.e.,

$$\begin{aligned} & \frac{L_{\text{dir}}(\lambda'_{\pm})\Omega(\Delta\theta)}{4\pi D^2} [1 - \exp(-\tau_{\text{rad}})] \{g(\mu) \exp(-\tau_{\text{off}}) + [1 - \exp(-\tau_{\text{off}})]\} \\ &= f_{\text{dir}}(\lambda'_{\pm})\Omega(\Delta\theta)[1 - \exp(-\tau_{\text{rad}})] \{g(\mu) \exp(-\tau_{\text{off}}) + [1 - \exp(-\tau_{\text{off}})]\} \quad , \quad (39) \end{aligned}$$

where we have used equation (17) from § 3.1. The total flux jet flux at Earth at wavelength

λ for the radial and optically-thin phases

$$f_{\text{radial/optically-thin}}(\lambda) = [f_{\text{dir}}(\lambda'_+) + f_{\text{dir}}(\lambda'_-)] \Omega_{\text{fr}}(\Delta\theta) [1 - \exp(-\tau_{\text{rad}})] \left\{ g(\mu) \exp(-\tau_{\text{off}}) + [1 - \exp(-\tau_{\text{off}})] \right\}. \quad (40)$$

Note that the $1 \mp \mu$ factors multiplying the direct fluxes that occur in the reflection phase expressions (see eq. [34] and [36] in § 3.3) do not appear in equations (39) and (40): in the ideal radial picture all parts of the jets send light to the observer and not just the Earth-side parts of the inner ends. The ideal radial phase is when $\tau_{\text{off}} \rightarrow 0$ or $\exp(-\tau_{\text{off}}) \rightarrow 1$: recall, the $\exp(-\tau_{\text{off}})$ and $1 - \exp(-\tau_{\text{off}})$ factors correct for the less-than-ideal radial picture situation.

In developing the equation (40), we are assumed the jets are not too closely aligned with the line of sight which would be at least approaching the occultation situation: as discussed in § 2, we are not concerning ourselves with the occultation situation in this paper.

From equation (40) and again making use of our understanding of equation (28) for the Rayleigh phase function (see § 3.3), we find that the net Stokes Q parameter for the observer-scattered flux is

$$Q_{\text{radial/optically-thin}}(\lambda) = [f_{\text{dir}}(\lambda'_+) + f_{\text{dir}}(\lambda'_-)] \Omega_{\text{fr}}(\Delta\theta) [1 - \exp(-\tau_{\text{rad}})] \left(\frac{3}{4} \right) (\mu^2 - 1) \exp(-\tau_{\text{off}}) \xi(\Delta\theta), \quad (41)$$

where we have again introduced the correction factor $\xi(\Delta\theta)$ (see eq. [26] in § 3.3) to account for the range of scattering planes. Note the $1 - \exp(-\tau_{\text{off}})$ term in equation (40) accounts for unpolarized flux, and thus the x - and y -fluxes it governs are equal and it cancels out of $Q_{\text{radial/optically-thin}}$.

3.5. General Expressions for All Phases

The flux and Stokes Q parameter expressions of §§ 3.3 and 3.4 were developed from idealized limiting-case pictures. The state of the jets in the times between when these pictures apply is complex, but it would be useful to have general expressions that cover the intermediate times as well. We will construct general expressions that are valid in the reflection and ideal radial/optically-thin phases and act as interpolation formulae for the intermediate times. (The ideal radial phase is when $\tau_{\text{off}} \rightarrow 0$ recall.) We are guided somewhat by an intermediate phase picture.

The reflection phase picture (see § 3.3) predicts that the fraction q of the photons incident on a jet undergo a single scattering and are highly polarized. The rest of the

photons (i.e., the fraction $1 - q$) are multiply scattered and emerge unpolarized (or rather randomly polarized and so yielding no net polarization). The radial phase ideally assumes that all scattered photons are scattered as if they had undergone a single scattering event and is therefore a more polarizing phase ideally. Less ideally, we estimate the polarized fraction of the escaping scattered photons is $\exp(-\tau_{\text{off}})$, where τ_{off} is the off-radial optical depth (i.e., the optical depth from the axis to the surface along a perpendicular to the axis) at the mean radial optical for the first scattering of a radial photon (i.e., at β_{scat}). We will argue that there can be no local minimum in polarization between the reflection and radial phases. First, it is plausible that the ratio of singly scattered to all scattered photons should be roughly constant as the reflection phase changes to the radial phase: both phases are optically thick in the radial direction and all photons are scattered: the photons just tend to penetrate more deeply as the jets expand with time. Just as the jet becomes optically thin perpendicular to the axis (i.e., $\tau_{\text{off}} \rightarrow 0$) the fraction of multiply scattered photons that are polarized (i.e., polarized in a non-random way) should increase from zero to all multiply scattered photons ideally: recall our description of the ideal radial phase scattering at the beginning of § 3.4. Now net polarization is set by the non-randomly polarized, scattered photons. Since these should increase in abundance as we go from the reflection phase to the ideal radial phase, we should expect polarization to increase monotonically.

We now can derive general expressions that handle the reflection and radial/optically-thin phases and interpolate between them. The discussion just above suggests replacing the q and $1 - q$ factors in the reflection phase equations for flux and Stokes Q parameter (see eq. [34] and [36] in § 3.3) and the $\exp(-\tau_{\text{off}})$ and $[1 - \exp(-\tau_{\text{off}})]$ factors in the counterpart radial/optically-thin phase expressions (see eq. [40] and [41] in § 3.4) by, respectively,

$$w = q + (1 - q) \exp(-\tau_{\text{off}}) = \begin{cases} q & \text{for } \tau_{\text{off}} \rightarrow \infty; \\ 1 & \text{for } \tau_{\text{off}} \rightarrow 0 \end{cases} \quad (42)$$

and

$$1 - w = (1 - q)[1 - \exp(-\tau_{\text{off}})] = \begin{cases} 1 - q & \text{for } \tau_{\text{off}} \rightarrow \infty; \\ 0 & \text{for } \tau_{\text{off}} \rightarrow 0, \end{cases} \quad (43)$$

since the change from reflection to radial phases can plausibly be identified as when τ_{off} drops below about 1. With these replacements the reflection phase and radial/optically-thin phase expressions become more alike. If we add a factor $[1 - \exp(-\tau_{\text{rad}})]$ to the reflection phase equations for flux and Stokes Q parameter, the expressions for the reflection and radial/optically-thin phases become identical, except for the $1 \mp \mu$ factors in the reflection phase expressions. To complete the general expressions, we must find away to smoothly change the $1 \mp \mu$ factors into 1's as the reflection phase changes to the radial/optically-thin phase.

The $(1 \mp \mu)$ factors were based on the very special, but heuristically useful, assumption that the inner ends of the jets could be treated as hemispheres with round sides toward the supernova center. We do not put much weight on this hemisphere assumption and have no strong guidance on how to effect the change from $1 \mp \mu$ factors to 1's as the reflection phase changes to the radial phase. Therefore, no elaborate procedure is warranted. One possibility is multiply the μ 's in the $1 \mp \mu$ factors by

$$w_\mu = \begin{cases} 1 - \frac{1}{\tau_{\text{off}}} & \text{for } \tau_{\text{off}} > 1; \\ 0 & \text{for } \tau_{\text{off}} \leq 1 \end{cases} \quad (44)$$

so that one has $1 \mp w_\mu \mu$ instead of $1 \mp \mu$ in the expression. The w_μ factor will give smooth transition between the phases and at what can be regarded as the characteristic end of the reflection phase when $\tau_{\text{off}} = 1$ the w_μ factor becomes a 0 and the $1 \mp \mu$ factors have effectively changed to exactly 1's.

One could, of course, devise alternative definitions of w_μ that change from 1 to 0 as the phases change. A very simple alternative is just to set $w_\mu = 0$ at all times. This simple alternative is warranted because we do not take the hemisphere assumption too seriously and also because the exact value $w_\mu \mu$ is not too important if $f_{\text{dir}}(\lambda'_+)$ and $f_{\text{dir}}(\lambda'_-)$ do not differ too much which may often be the case. Also in actual cases where polarization is high, μ is likely to be closer to 0 than to 1 which would tend to make the exact value of w_μ of little importance.

Below we will insert w_μ factors to account for the transition of $1 \mp \mu$ factors to 1's, but we make no final specification of w_μ factors. In all our demonstration calculations in § 4, we take $\theta = 90^\circ$ (i.e., $\mu = 0$) and the value of w_μ factors is irrelevant.

Making all the changes to the expressions for the reflection and radial/optically-thin phases that we suggested above and replacing $1 \mp \mu$ by $1 \mp w_\mu \mu$ in the reflection phase expressions and inserting $1 \mp w_\mu \mu$ in the radial/optically-thin phases appropriately, makes the reflection and radial/optically-thin phase expressions identical and these identical expressions are our general expressions for the jet-scattered flux and its Stokes Q parameter. Explicitly, the general expressions are

$$f_{\text{jet}}(\lambda) = [f_{\text{dir}}(\lambda'_+)(1 - w_\mu \mu) + f_{\text{dir}}(\lambda'_-)(1 + w_\mu \mu)] \Omega_{\text{fr}}(\Delta\theta) [1 - \exp(-\tau_{\text{rad}})] [g(\mu)w + (1 - w)] \quad (45)$$

and

$$Q_{\text{jet}}(\lambda) = [f_{\text{dir}}(\lambda'_+)(1 - w_\mu \mu) + f_{\text{dir}}(\lambda'_-)(1 + w_\mu \mu)] \Omega_{\text{fr}}(\Delta\theta) [1 - \exp(-\tau_{\text{rad}})] \left(\frac{3}{4}\right) (\mu^2 - 1) w \xi(\Delta\theta) . \quad (46)$$

These expressions interpolate smoothly between the reflection phase and the ideal radial phase (where $\tau_{\text{off}} \rightarrow 0$) and also handle the optically-thin phase, of course. This can be seen by comparing in detail the expressions to equations (34) and (36) in § 3.3 and equations (40) and (41) in § 3.4.

For actual analysis we would like the ratio R of jet-scattered to direct flux (which we call the relative scattered flux) and the polarization expression for the total flux. Dividing equation (45) by $f_{\text{dir}}(\lambda)$ gives the relative scattered flux

$$R(\lambda) = \frac{f_{\text{jet}}(\lambda)}{f_{\text{dir}}(\lambda)} = \left[\frac{f_{\text{dir}}(\lambda'_+)(1 - w_\mu\mu) + f_{\text{dir}}(\lambda'_-)(1 + w_\mu\mu)}{f_{\text{dir}}(\lambda)} \right] \Omega_{\text{fr}}(\Delta\theta) [1 - \exp(-\tau_{\text{rad}})] [g(\mu)w + (1 - w)] . \quad (47)$$

For polarization we divide the absolute value of the $Q_{\text{jet}}(\lambda)$ expression by total flux $f_{\text{dir}}(\lambda)[1 + R(\lambda)]$ and multiply by 100 % since polarization is conventionally given as a percentage:

$$P(\lambda) = \left[\frac{f_{\text{dir}}(\lambda'_+)(1 - w_\mu\mu) + f_{\text{dir}}(\lambda'_-)(1 + w_\mu\mu)}{f_{\text{dir}}(\lambda)[1 + R(\lambda)]} \right] \Omega_{\text{fr}}(\Delta\theta) [1 - \exp(-\tau_{\text{rad}})] \left(\frac{3}{4} \right) (1 - \mu^2) w \xi(\Delta\theta) \times 100 \% . \quad (48)$$

Recall we assume that the direct supernova flux is unpolarized and therefore has zero Stokes Q parameter: thus equation (48) gives the total supernova polarization for the bipolar jet model. The $1/[1 + R(\lambda)]$ factor in the polarization expression is probably usually negligibly different from 1 for cases where our approximations are best: i.e., when jets subtend relatively little solid angle (i.e., when $\Omega_{\text{fr}}(\Delta\theta)$ is small), and thus are relatively narrow and scatter relatively little flux.

If one is trying to obtain R and P from observed flux, then one can substitute $f_{\text{obs}}(\lambda)/[1 + R(\lambda)]$, $f_{\text{obs}}(\lambda'_+)/[1 + R(\lambda'_+)]$, and $f_{\text{obs}}(\lambda'_-)/[1 + R(\lambda'_-)]$ into equations (47) and (48) for $f_{\text{dir}}(\lambda)$, $f_{\text{dir}}(\lambda'_+)$, and $f_{\text{dir}}(\lambda'_-)$, respectively. Usually one can then drop the inserted $1/(1 + R)$ factors as being negligible and then no complex solution for R as a function of wavelength is required. In fact, the inserted $1/(1 + R)$ factors probably often partially cancel out of the equations: they exactly cancel out if R is constant with wavelength. A case where R might become large and where a complex solution might be needed for high accuracy is in the trough features of P Cygni lines where $f_{\text{dir}}(\lambda)$ becomes small while $[f_{\text{dir}}(\lambda'_+) + f_{\text{dir}}(\lambda'_-)]$ could stay large due to the redshift effect. But given that the bipolar jet model is crude, complex solutions for R are probably a waste of effort almost always.

Our general expressions for R and polarization P depend on 5 independent basic parameters: θ (the angle of the jet axis from the line of sight) or $\mu = \cos \theta$, $\Delta\theta$ (the half-opening

angle of the jets), β_{in} (the inner end of the jet in velocity), $b = \Delta\beta_{\text{rad}}/\beta_{\text{in}}$ (the ratio of jet velocity length to inner end velocity of jet), and τ_{rad} (or if the time-delay effect is included t_{red} : see § 3.2). The τ_{rad} parameter can be resolved into time t and the $\tau_{\text{rad},0}t_0^2$ parameter (see eq. [9] in § 2) for an analysis of the time evolution of polarization: in this case $\tau_{\text{rad},0}t_0^2$ replaces τ_{rad} as one of the 5 independent basic parameters. The q parameter, which is an argument of the w factor (see eq. [42] and [43] above) is also independent, but we consider its value as fixed at 1/4 (see § 3.3, esp. eq. [23]), and so exclude it from our list of independent basic parameters. The non-basic parameters in the R and P depend on the basic parameters as follows: λ'_{\pm} depends on θ , β_{in} , b , and τ_{rad} (see eq. [13] and [14] in § 2 and eq. [30] in § 3.3); w depends on $\Delta\theta$, b , and τ_{rad} (and on q too) (see eq. [13] and [15] in § 2 and eq. [42] and [43] above); w_{μ} using our first prescription depends on $\Delta\theta$, b , and τ_{rad} , (see eq. [13] and [15] in § 2 and eq. [44] above) and on nothing if we set it to zero.

Given the 5 independent basic parameters, one can correct the synthetic supernova spectrum $f_{\text{dir}}(\lambda)$ of any spherically symmetric calculation to include the additional flux from a jet by multiplying this spectrum by $1 + R$, where R itself is evaluated using the synthetic $f_{\text{dir}}(\lambda)$. An observed spectrum (which naturally includes jet flux if there are jets) can be corrected to the direct supernova spectrum by dividing by $1 + R$ or multiplying by $1 - R$ assuming R small. In this case, R is evaluated using the observed $f_{\text{obs}}(\lambda)$ (as discussed above) which, of course, includes jet flux if there is any: this, however, gives a direct flux that is first order correct in small R .

There is considerable degeneracy among the 5 independent basic parameters and finding a uniquely good set for a single continuum polarization observation would be difficult. A fit to an observed time evolution of continuum polarization may break some of the degeneracy.

For example, consider θ and $\Delta\theta$. The polarization increases with θ up to θ 's maximum value of 90° degrees through the $1 - \mu^2$ factor. But the polarization also scales with $\Omega_{\text{fr}}(\Delta\theta)\xi(\Delta\theta)$ which is the most obvious manifestation of the $\Delta\theta$ parameter: $\Omega_{\text{fr}}(\Delta\theta)\xi(\Delta\theta)$ increases with $\Delta\theta$ from zero for $\Delta\theta = 0^\circ$ to a maximum of 0.1046 at $\Delta\theta \approx 56.48^\circ$ (which is beyond where our picture of a narrow jet has plausible validity) and then decreases with $\Delta\theta$ to zero at $\Delta\theta = 90^\circ$. Clearly, θ and $\Delta\theta$ could be varied in a compensating way while holding the polarization constant or nearly. Thus, there is a strong time-independent degeneracy between θ and $\Delta\theta$.

Now $\Delta\theta$ also affects the w factor (see eq. [42] above) through the τ_{off} optical depth (see eq. [15] in § 2). Since w varies in time due to the time variation of τ_{rad} (see eq. [13] and [15] in § 2), the degeneracy of $\Delta\theta$ and θ may be broken by fitting to an observed time evolution of continuum polarization. However, two other parameters come into τ_{off} : b (see eq. [15] in § 2) and $\tau_{\text{rad},0}t_0^2$ (which replaces τ_{rad} as an independent basic parameter in a time-dependent

calculation) (see eq. [9] in § 2), and these can be used to compensate variations in $\Delta\theta$ to some degree. The situation is further complicated by the fact that the time variation of τ_{rad} also directly affects the polarization through the $1 - \exp(-\tau_{\text{rad}})$ factor.

Clearly, even when studying an observed time evolution of continuum polarization, parameter degeneracy will be a problem in finding a uniquely good set of the 5 independent basic parameters. Any constraints on the jet structure from non-polarimetric observations or theory would help to break the degeneracy.

Another parameter degeneracy example involves the redshift effect. The redshift effect depends on θ (through μ) and β_{scat} (see eq. [30] in § 3.3). Now β_{scat} depends on b , β_{in} , and τ_{rad} (see eq. [13] and [14] in § 2). The redshift effect manifests itself most prominently in polarization spectra: we study this manifestation in § 4.3 and 4.4. If θ , b , and τ_{rad} can be determined from the time evolution of the continuum polarization then that breaks the degeneracy with β_{in} which can be determined from analysis of polarization spectra since β_{in} has a strong effect on the redshift effect (see eq. [14] in § 2 and eq. [30] in § 3.3).

Even if a unique set of the 5 independent basic parameters cannot be obtained from polarimetric observations, it would still be very interesting if the bipolar jet model could be shown to be adequate for those observations.

4. Demonstration Calculations

In this section, we present demonstration calculations for continuum polarization and polarization spectra. In the continuum polarization case, it is of especial interest to see if the bipolar jet model can yield a continuum polarization time evolution that rises to a maximum and then declines with time (see § 4.2) and if it can yield the inverted P Cygni polarization profiles of lines (see §§ 4.3 and 4.4).

For simplicity we neglect the time-delay effect (see § 3.2) in all our calculations. This means that we use a single reduced time t_{red} (which specifies the radial optical depth τ_{rad} through eq. [10] in § 2) to calculate the polarization for each epoch or we use τ_{rad} as one of the independent basic parameters. Also in all our calculations, we set $\theta = 90^\circ$ (i.e., the jets are aligned perpendicular to the line of sight): recall θ is one of the 5 independent basic parameters (see § 3.5). This θ is the maximally polarizing choice as one can see from equation (48) in § 3.5, where the main θ dependence is through $1 - \mu^2$ where $\mu = \cos\theta$. (The θ parameter also affects the polarization through the redshift effect: see equation [30] in § 3.3.)

In § 4.1 we consider continuum polarization with varying $\Delta\theta$ and in § 4.2 continuum polarization as a function of time. In § 4.3, we discuss polarization line and continuum features. Synthetic polarization spectrum calculations are presented in § 4.4.

4.1. Continuum Polarization Calculations with Varying $\Delta\theta$

For the strictly continuum polarization calculations in this subsection and § 4.2, we assume the direct flux from the bulk supernova is constant with wavelength: this is the neutral choice. Thus we have $f_{\text{dir}}(\lambda'_+) = f_{\text{dir}}(\lambda'_-) = f_{\text{dir}}(\lambda)$ for these calculations and in equation (48) in § 3.5 the factor

$$\frac{f_{\text{dir}}(\lambda'_+)(1 - \omega_\mu\mu) + f_{\text{dir}}(\lambda'_-)(1 + \omega_\mu\mu)}{f_{\text{dir}}(\lambda)} = 2 \quad (49)$$

note that the values of ω_μ and μ are irrelevant in the flux ratio factor for a constant continuum flux. The assumption of wavelength-independent direct flux effectively eliminates the redshift effect from the calculations (see eq. [30] in § 3.3). This means that the independent basic parameter β_{in} and the dependent parameter β_{scat} (see eq. [14] in § 2) never come into the calculations. Thus, we do not specify values of β_{in} in this section or in § 4.2.

In this subsection, we are interested in seeing how continuum polarization varies with $\Delta\theta$ with other parameters chosen for a high polarization case in the radial phase. To get a large polarization we set $b = \infty$ (which makes the jets infinitely long compared to distance from the supernova center to inner jet surface: see eq. [4] in § 2) and $\tau_{\text{rad}} \gg 1$ (which means all photons entering the jet are scattered). These choices make $\tau_{\text{rad}}/b = 0$, $\tau_{\text{mean}} = 1$, and $\tau_{\text{off}} = \Delta\theta$ (see eq. [13] and [15] in § 2) and $1 - \exp(-\tau_{\text{rad}}) \approx 1$: a fairly small τ_{off} and $1 - \exp(-\tau_{\text{rad}})$ nearly 1 produce high polarization (see eq. [48] and [42] in § 3.3). (As we will show in Figure 1 in § 4.2, slightly, but distinctly, higher continuum polarizations than for $\tau_{\text{rad}} \gg 1$ can be achieved for $b = \infty$ and $\Delta\theta \gtrsim 30^\circ$ as τ_{rad} declines with time toward the neighborhood of 1.)

For the specified 3 independent basic parameters (e.g., $\theta = 90^\circ$, $b = \infty$, and $\tau_{\text{rad}} \gg 1$) and independent basic parameter β_{in} unspecified since it is irrelevant, Table 1 shows, as a function of the independent basic parameter $\Delta\theta$, the runs of $\Omega_{\text{fr}}(\Delta\theta)$, $\xi(\Delta\theta)$, w , R , and polarization P . Equation (48) in § 3.5 shows how polarization depends on the dependent parameters $\Omega_{\text{fr}}(\Delta\theta)$, $\xi(\Delta\theta)$, w , and R in a direct sense. The competing effects of $\Delta\theta$ through the dependent parameters yield a polarization maximum of about 6.63% at $\Delta\theta \approx 45.6^\circ$. This opening angle is beyond where our picture of a narrow jet has plausibility. However a continuum polarization of 4% is reached at $\Delta\theta \approx 24^\circ$ which is plausibly still a sufficiently

narrow jet to channel non-escaping photons mostly radially as in our ideal picture of the radial phase discussed in § 3.4.

The polarization result of 4 % just mentioned is encouraging for the bipolar jet model if it turns out that polarization of this size (which is possibly the current record continuum polarization for a supernova: see § 1.1) is required from the model to fit observations. However, the result is obtained with high-polarizing choices for θ , b , and τ_{rad} . For example if we make $b = 0$, the jets become geometrically short along their axis: the radial channeling effect of non-escaping scattered photons disappears. The jets in this case remain in the reflection phase with $\tau_{\text{off}} = \infty$ and $w = q = 1/4$ (see eq. [15] in § 2 and eq. [42] in § 3.5 and eq. [23] in § 3.3) until they become optically thin radially. (Having $w = 1/4$ when the jets becomes radially optically thin is an unphysical limiting case for the equation [48] since most photons that scatter once will escape without being scattered again and therefore will not be depolarized by multiple scattering as $w = 1/4$ implies.) Much lower polarizations than in the $b = \infty$ case would be found since every explicit factor in equation (48) is the same as for the $b = 0$ case, except that w is distinctly smaller (i.e., $w = 1/4$ as compared to the w values in Table 1) which distinctly decreases polarization and that R increases a bit which is because of smaller w and slightly decreases polarization. With fiducial parameters used in Table 1, except that b is chosen to be 0, the continuum polarization reaches a maximum of only about 2.8 % for $\Delta\theta = 51^\circ$. For $\Delta\theta = 24^\circ$, the polarization is only 1.3 %.

The effect of the b parameter on the time evolution of the polarization is significant. As long as $\Delta\theta\tau_{\text{rad}}/b$ (with $\Delta\theta$ in radians, of course) is large, the off-radial escape of highly polarized photons, except for reflected photons the inner end of the jet, is small. Recall this escape is governed in the model by $\exp(-\tau_{\text{off}})$ (see eq. [42] and [43] in § 3.5), where $\tau_{\text{off}} = \Delta\theta(\tau_{\text{rad}}/b + \tau_{\text{mean}})$ (see eq. [15] in § 2). Only when τ_{off} becomes less than of order 1 while τ_{rad} is still significantly larger than 1 does the ideal radial phase high polarizing effect that was discussed in § 3.4 begin to be approached. However, if τ_{rad} is falling below 1 when τ_{off} becomes of order 1, then polarization could start falling because a decreasing number of photons are scattered at all in the jet. Thus, we expect localized polarization maxima in time evolution when $\tau_{\text{off}} \lesssim 1$ (requiring $\Delta\theta\tau_{\text{rad}}/b \lesssim 1$), but $\tau_{\text{rad}} \gtrsim 1$. Our calculations bear this out: see § 4.2, esp. Fig. 2.

4.2. Calculations of Continuum Polarization as a Function of Time

In Figures 1, 2, and 3, we show the time evolution of the continuum polarization for representative b values and $\Delta\theta$ values with $\theta = 90^\circ$. Since we are assuming a wavelength-independent direct supernova flux as in § 4.1, $[f_{\text{dir}}(\lambda'_+)(1 - w_\mu\mu) + f_{\text{dir}}(\lambda'_-)(1 + w_\mu\mu)]/f_{\text{dir}}(\lambda) =$

2 and β_{in} is unspecified since it is irrelevant for a wavelength-independent direct supernova flux. The time used is the reduced time $t_{\text{red}} = 1/\sqrt{\tau_{\text{rad}}}$ (see § 2, esp. eq. [10]) which eliminates the need to specify a $\tau_{\text{rad},0}t_0^2$ parameter (see eq. [9] in § 2).

Figure 1 shows the $b = 0$ cases (solid lines) and $b = \infty$ cases (dashed lines) for a range of $\Delta\theta$ values including 46° which yields near maximum polarization for the $b = \infty$ case (see Table 1). The only difference between the $b = 0$ and $b = \infty$ cases is that in the former $w = q = 1/4$ for all times and in the latter $w = q + (1 - q)\exp(-\Delta\theta\tau_{\text{mean}})$ (see eq. [13] and [15] in § 2, eq. [23] in § 3.3, and eq. [42] in § 3.5). In the $b = \infty$ cases, w will rise monotonically from $w = q + (1 - q)\exp(-\Delta\theta)$ at early times (when $\tau_{\text{rad}} \gg 1$ and $\tau_{\text{mean}} = 1$: see eq. [13] and [15] in § 2) to 1 at late times (when $\tau_{\text{mean}} \rightarrow 0$): w in the $b = \infty$ cases will always be greater than $q = 1/4$.

The early time behavior of the $b = 0$ cases is the first kind of polarization plateau phase discussed at the end of § 2. The early time behavior of the $b = \infty$ cases is the second kind of polarization plateau phase likewise discussed at the end of § 2. The first kind of plateau phase is unavoidable and should be observable if a supernova with jets of the kind we have posited is observed early enough. The second kind can only exist if $b \gg 2$, and is probably physically unrealizable for cases of significant polarization as we discuss below.

A representative set of the Table 1 predictions for $b = \infty$ with $\tau_{\text{rad}} \gg 1$ are illustrated by the $b = \infty$ cases in Figure 1 at times t_{red} significantly less than 1. As mentioned in § 4.1, the $b = \infty$ cases can actually rise slightly, but distinctly, above the Table 1 predictions for $\Delta\theta \gtrsim 30^\circ$ when τ_{rad} declines toward the neighborhood of 1: the actual localized maxima in the figure occur at $t_{\text{red}} \approx 0.54$ ($\tau_{\text{rad}} \approx 3.5$) for $\Delta\theta = 30^\circ$ and at $t_{\text{red}} \approx 0.66$ ($\tau_{\text{rad}} \approx 2.3$) for $\Delta\theta = 46^\circ$. Declining τ_{rad} tends to lower polarization by reducing the number of photons scattered in the jet. But, as discussed in § 4.1, the competing effect of declining τ_{off} (which increases w and thus tends to increase polarization) briefly dominates and the ideal radial phase high polarizing effect is approached. The calculations show that this situation causes distinct polarization maxima to appear for sufficiently large $\Delta\theta$. The $b = 0$ cases are at all times lower in polarization than the $b = \infty$ cases of the same $\Delta\theta$ because the $b = 0$ case w factor is everywhere smaller, except all cases have zero polarization when $t_{\text{red}} = \infty$. The $b = 0$ cases decline monotonically with t_{red} : their only time dependence comes through the $1 - \exp(-\tau_{\text{rad}})$ factor which declines monotonically with time (see § 3.5, eq. [48]).

Figure 2 shows the $b = 1$ and $b = 3$ cases for the same $\Delta\theta$ values as used for Figure 1. These cases further illustrate the effect of the b parameter on the time evolution. As long as $\Delta\theta\tau_{\text{rad}}/b \gg 1$ (i.e., at early times with $\Delta\theta$ in radians, of course), the off-radial escape of highly polarized photons is small and the polarization is just as in the $b = 0$ case: i.e., $\tau_{\text{off}} \gg 1$, and so $w = q = 1/4$. This early phase is the first kind of polarization plateau

phase discussed at the end of § 2.

When $\Delta\theta\tau_{\text{rad}}/b$ becomes small the ideal radial phase effect become high and polarization begins to rise. However, sometime thereafter τ_{rad} becomes small and the polarization falls as overall scattering declines. Thus, we expect, as discussed at the end of § 4.1, a polarization maximum in time evolution when $\Delta\theta\tau_{\text{rad}}/b \lesssim 1$ (i.e., there is high off-radial escape probability for polarized photons), but $\tau_{\text{rad}} \gtrsim 1$ (i.e., there is still strong scattering in the jet). Figure 2 shows this is the case. Note the polarization maxima are higher and shifted to earlier times for the $b = 3$ cases relative to the corresponding $b = 1$ cases: this is because for the $b = 3$ cases there are longer time periods starting earlier where the conditions $\Delta\theta\tau_{\text{rad}}/b \lesssim 1$ and $\tau_{\text{rad}} \gtrsim 1$ hold and a greater degree of the ideal radial phase effect is reached. Note also that though polarization increases with greater $\Delta\theta$, increased $\Delta\theta$ tends to shift the polarization maxima to later times because again the condition $\Delta\theta\tau_{\text{rad}}/b \lesssim 1$ has to be approximately met for the maxima to occur.

The maxima in Figure 2 do not reach the high polarizations and the second kind of polarization plateaus obtained for corresponding $b = \infty$ cases (see Fig. 1) which shows that there is never a time when $\Delta\theta\tau_{\text{rad}}/b$ is negligible in the evaluation of τ_{off} while $\tau_{\text{rad}} \gtrsim 1$. For instance, the $b = 3$, $\Delta\theta = 30^\circ$ case reaches a maximum polarization of 4.06 % at $t_{\text{red}} = 0.74$ whereas the $b = \infty$, $\Delta\theta = 30^\circ$ case had polarization greater than 5 % for $t_{\text{red}} \lesssim 0.75$.

The prediction of a period of rising polarization with time given by the calculations for Figure 2 is qualitatively in agreement with the observations of SN 1987A (Jeffery 1991b) and SN 1999em (Leonard et al. 2001). The prediction of eventual decline of intrinsic polarization to a very low level is believed to be in agreement with observations for SN 1987A (Méndez 1990; Jeffery 1991b). An eventual decline in supernova polarization with time must occur in any model depending on electron scattering polarization since the electron optical depth must decline eventually as the supernova ejecta expands. Our polarization expression (eq. [48] in § 3.5) predicts that in all cases polarization will start to fall when τ_{rad} declines to of order 1.

Recall $\sim 4\%$ polarization is a possible record for continuum polarization for a core-collapse supernova (see § 1.1). The $b = 3$, $\Delta\theta = 30^\circ$ jet polarization shown in Figure 2 reaches level. We consider bipolar jets with these parameters a physically plausible case in which the jets are relatively narrow. It is satisfying that a plausible bipolar jet case can reach the possible record polarization.

In Figure 3, we show the polarization time evolution curves for $\Delta\theta = 10^\circ$ and a range of b values from 0 to infinity. As we would expect from our discussion of the Figure 2 curves above, the polarization maxima in Figure 3 get higher and broader as b is increased since the time period of $\Delta\theta\tau_{\text{rad}}/b$ small while $\tau_{\text{rad}} \gtrsim 1$ is longer and there is a stronger ideal radial

phase effect. For $b \gtrsim 100$, there is the second kind of polarization plateau.

Physically b values over 50 are probably impossible since they give $\Delta\beta_{\text{rad}} = \beta_{\text{in}}b > 1$ (i.e., outer end jet speeds greater than light) even for modest $\beta_{\text{in}} = 0.02$ (i.e., jet inner end speed of about 6000 km/s) which is of order of the velocity of supernova photospheres for much of the observable epoch. (Recall as $\Delta\beta_{\text{rad}}$ becomes more relativistic our treatment becomes less adequate because we have neglected relativistic effects in our formalism and because in the present calculations we are neglecting the time-delay effect.) Reducing $\Delta\theta$ allows the second kind of polarization plateau to be reached with smaller b values. For example, $\Delta\theta = 1^\circ$ in calculations otherwise like those of Figure 3 causes the polarization plateau to appear for $b \gtrsim 10$, but, as one would expect from equation (2) (§ 2) and equation (48) (§ 3.5), the polarization scales down everywhere by a factor of about 100 from the Figure 3 calculations: the $\Delta\theta = 1^\circ$ curves have polarizations of order 0.01 % or less which are currently observationally insignificant. (We believe that typically the lower limit of observationally significant polarization is perhaps 0.1 %. Depending on circumstances the lower limit could vary up and down from this, of course.)

The upshot of the discussion in last paragraph is that the second kind of polarization plateau which is evident in Figures 1 and 3 is probably not physically realizable for high polarization cases. It seems unlikely that the inclusion of full relativistic effects and time-delay effects will ease the requirement for very high b values in order to get the second kind of polarization plateau for cases of significant continuum polarization. Thus the second kind of polarization plateau is only a mathematical prediction of the bipolar jet model for cases of significant continuum polarization. We do not expect it to be observed. Consequently, the very large and infinite b value cases seen in Figure 3 and the infinite b value cases of Figure 1 only illustrate mathematical trends of the bipolar jet model formalism.

The other extreme from large b is when b is decreased toward zero (see Fig. 3 again). In this situation, the localized polarization maximum that can occur near $t_{\text{red}} = 1$ (i.e., $\tau_{\text{rad}} = 1$) can first cease to be a global maximum (see the $b = 0.1$ curve) and then can disappear altogether (see the $b = 0.01$ curve) as b is reduced.

Figure 3 also illustrates that all curves approach the same functional behavior at late times where they decline like $\tau_{\text{rad}} = t_{\text{red}}^{-2}$ (see eq. [10] in § 2) since $1 - \exp(-\tau_{\text{rad}}) \rightarrow \tau_{\text{rad}}$ at late times. The late-time asymptotic curve is the same for all cases, except for the $b = 0$ curve. This is because for $b > 0$, the τ_{off} quantity goes to zero as time increases, and thus w goes to 1 as time increases (see eq. [13] and [15] in § 2 and eq. [42] and [48] in § 3.5). The $b = 0$ curve does not approach the same asymptotic curve because τ_{off} is always infinite, and thus $w = q = 1/4$ for all times.

The continuum polarization calculations we have done here have been to demonstrate the range of polarization behaviors that might be expected from supernovae with bipolar jets and to illustrate the mathematical properties of the polarization formula (eq. [48] in § 3.5). If one had observed continuum polarization as function of time (i.e., real time, not reduced time), a fit to the observations could be done to determine values for θ , $\Delta\theta$, b , and the $\tau_{\text{rad}}t_0^2$ parameter (see § 2, eq. [9]). Unfortunately, the degeneracy of the parameters which we discussed at the end of § 3.5 would make it difficult to determine a unique set of parameters.

4.3. Polarization Line and Continuum Features

Polarization spectra would have exactly constant polarization without the redshift effect of the jets (see § 3.3, esp. eq. [30]). With the redshift effect, P Cygni line flux features tend to give rise to inverted P Cygni polarization profiles: high polarization at the blueshifted trough of P Cygni flux profile and low polarization at the near-line center maximum of a P Cygni flux profile. This kind of line polarization profile is also produced by other supernova polarization models (see § 1.1 for other supernova polarization models) and is, in fact, present or partially present for some observed supernova P Cygni lines (e.g., Jeffery 1991b, Wang et al. 2001, and Leonard et al. 2001). That the bipolar jet model can yield such a profile is a success. However, the observed profiles often show shifts in position angle which the strictly axisymmetric bipolar jet model cannot yield. Thus, the axisymmetric bipolar jet asymmetry even if it exists cannot be the only asymmetry in many cases and maybe in all cases.

The inverted P Cygni profiles in the bipolar jet model arise as follows. Because of the redshift effect the jet-scattered, polarized flux originates in direct flux spectrum from a bluer part of that spectrum than the part of that spectrum to which it (i.e., the jet-scattered, polarized flux) is added to make up the total flux spectrum. Now if this bluer flux is redshifted from a continuum region to another continuum region there will be a certain scattered flux to direct flux ratio and a certain polarization in the second region. If the bluer flux is redshifted from a continuum region to P Cygni trough region, then there will be a higher scattered flux to direct flux ratio and higher polarization in the second region: the higher polarization is because there is less dilution of the scattered, polarized flux by unpolarized direct flux. If the bluer flux is redshifted from a continuum region to P Cygni emission peak region, then there will be a lower scattered flux to direct flux ratio and lower polarization in the second region: the lower polarization is because there is more dilution of the scattered, polarized flux by unpolarized direct flux. The net result of scattered continuum flux redshifted to a P Cygni line, is an inverted P Cygni polarization profile associated with P Cygni flux profile: higher than continuum polarization in the trough region; lower than continuum polarization

in the emission region.

Now P Cygni line widths are caused by Doppler shifts on scattering in the fast moving ejecta at and beyond the photosphere: the Doppler shifts correspond typically to velocities of order 1 or 2 times the photospheric velocity β_{ph} : the shifts can be larger for very strong lines. Since we assume the jets and their main scattering region at β_{scat} to be well outside the photosphere (i.e., $\beta_{\text{scat}} \gg \beta_{\text{ph}}$), the jet redshift is usually going to be larger than the typical P Cygni line width. Thus, jet-scattered flux redshifted into a P Cygni line wavelength region will usually come from an unrelated bluer part of the spectrum which could be continuum or could be complicated by other P Cygni lines possibly overlapping each other. But if the P Cygni line is a strong one, then usually the redshifted, jet-scattered flux that is added to it will be more continuum-like than the P Cygni line itself. Thus for strong P Cygni lines or P Cygni lines sufficiently well isolated by continuum regions, one usually expects inverted P Cygni polarization profiles by the mechanism discussed in the last paragraph. Admittedly, a complex direct flux spectrum with many overlapping P Cygni will give rise to a complex polarization spectrum in which the inverted P Cygni profiles might not be clearly present.

Purely continuum polarization features can arise if the jet is very fast: i.e., $\beta_{\text{scat}} \gg \beta_{\text{ph}}$. This is because there will be very large redshifts and variations in the direct flux continuum level will affect the polarization spectrum. For example, say that the jet redshift moves direct flux from the ultraviolet (UV) region to the blue part of the optical and from the blue part to the red part of the optical. Now the UV flux of a supernova is very low compared to the optical in the observable epoch after very early times because of strong line-blanketing. In this case, the jet-scattered UV flux that is redshifted into the blue part of the optical will be comparatively very low and even if highly polarized might be insufficient to cause significant polarization of the net flux. On the other hand, in the red part of the optical, the polarization should be higher than in the blue part since the jet-scattered flux from the blue part is shifted there. Thus, polarization should rise strongly across the optical in this example situation.

4.4. Polarization Spectrum Calculations

Using the expressions for relative flux R and polarization P (eq. [47] and [48] in § 3.5) and a set of the 5 independent basic parameters for the bipolar jet model, one can calculate the direct-plus-jet spectrum and polarization spectrum for any synthetic spectrum calculated in spherical symmetry. One can also take any observed flux spectrum and a set of the 5 independent basic parameters and calculate a direct spectrum (see § 3.5 for the method) and a polarization spectrum. If one has an observed polarization spectrum, one can do a

fit to that spectrum by adjusting the parameters. Unfortunately, the effect of parameters is very degenerate since they combine in a complex way to control the level of polarization as discussed at the end of § 3.5. An analysis of the time evolution of the continuum polarization might allow one to at least partially break the degeneracy and obtain values for θ , $\Delta\theta$, b , and $\tau_{\text{rad},0}t_0^2$ (see § 3.5 and 4.2). An analysis of the polarization spectrum would then allow a determination of β_{in} parameter since it has a strong effect on the redshift effect (see eq. [14] in § 2 and eq. [30] in § 3.3).

As a demonstration we have calculated the direct spectrum and polarization spectrum for an observed spectrum of SN Ib 1999dn (in NGC 7714) from 17 days after V maximum (i.e., about 37 days after explosion assuming a rise time of about 20 days: see § 1.2). The observed spectrum is from Matheson et al. (2001). The photospheric velocity β_{ph} of the supernova at that epoch was 0.02 (i.e., $v_{\text{ph}} = 6000 \text{ km/s}$) (BBK). For the 5 independent basic parameters we have chosen $\theta = 90\%$ (for simplicity and high polarization), $\Delta\theta = 20\%$ (for high polarization and yet still to have a relatively narrow jet: it is also the fiducial value from § 2), $b = 1$ (for simplicity: it is also our fiducial value from § 2), $\beta_{\text{in}} = 0.06$ (for simplicity since it is exactly 3 times the photospheric velocity and also for a significant redshift effect), and $\tau_{\text{rad}} = 0.67455$ (for relatively high polarization in the radial phase of the jets and to obtain the fiducial mass of § 2: see below).

The dependent parameters implied by the independent basic parameters are $t_{\text{red}} = 1.2176$, $\tau_{\text{mean}} = 0.300$, $\Delta\beta_{\text{rad}} = 0.06$, $\tau_{\text{off}} = 0.340$, and $\beta_{\text{scat}} = 0.0867$. Note $\omega_{\mu} = 0$ for $\tau_{\text{off}} \leq 1$ by our prescription equation (44) (§ 3.5), but its value is irrelevant since $\theta = 90\%$ (see eq. [48] in § 3.5). If we neglect the redshift effect and set $[f_{\text{dir}}(\lambda'_+)(1 - w_{\mu}\mu) + f_{\text{dir}}(\lambda'_-)(1 + w_{\mu}\mu)]/f_{\text{dir}}(\lambda) = 2$, R and polarization are, respectively, 0.0238 and 1.56%: these are characteristic R and polarization values for the calculation. Interpolating from Figure 2, we know for the specified τ_{rad} and reduced time that the continuum polarization would be declining from its time evolution maximum.

If we choose $\mu_e = 4$ and $t = 37$ days, then equations (7) and (8) (§ 2) imply that each jet has mass $0.1 M_{\odot}$ and characteristic kinetic energy $0.724 \times 10^{51} \text{ ergs} = 0.724 \text{ foe}$. This mass and kinetic energy were the fiducial jet values of § 2 and our choice of precisely 0.67455 for τ_{rad} was made to yield them.

Figure 4 shows the observed flux spectrum and the calculated direct flux spectrum. The direct spectrum was calculated using a R value which in turn was calculated from the observed flux by the method suggested in § 3.5. Since the characteristic R value for the calculation is small (0.0238: see above), this method is quite accurate. The scale of the spectra is arbitrary. The spectra have been corrected for the redshift due to the host galaxy heliocentric velocity (2798 km/s) and for the host galaxy Galactic foreground reddening

($E_{B-V}=0.052$) using the reddening law of Cardelli et al. (1989) with the revision of O’Donnell (1994). Both host galaxy correction parameters were obtained from the NED database (<http://nedwww.ipac.caltech.edu/>).

Since the direct spectrum is on average only about 2.4 % lower than the observed spectrum, the two spectra virtually overlap. The effect of the jet-scattered flux on the observed spectrum is probably negligible compared to observational error. Having a negligible effect on an observed spectrum at the same time as producing significant polarization was, of course, a main desideratum from the bipolar jet model since this desideratum would resolve the potential paradox discussed in § 1.2.

Figure 5 shows the calculated bipolar jet model polarization spectrum overlaid on the observed flux spectrum. Note that the polarization spectrum can only extend as far to the blue as the jet-redshifted blue end of the flux spectrum. Inverted P Cygni polarization profiles associated with flux spectrum P Cygni lines are evident: the one associated with the H and K Ca II P Cygni line (trough centered at $\sim 3750 \text{ \AA}$) is the most clear example. The line blending in the flux spectrum, of course, somewhat distorts the inverted P Cygni polarization profiles. The largest polarization maxima, not counting the far red end of the spectrum, reach over 4 %. The complex high polarization features at the red end of the spectrum rise higher: the highest is about 9 %. We cut off these high polarization features in the figure to preserve the clarity of the rest of the polarization spectrum. In any case, the red end of the flux spectrum from which these high polarization features are partially determined is probably uncertain.

For Figure 6, we have changed the independent basic parameter β_{in} to 0.12. The changed dependent parameters are $\Delta\beta_{\text{rad}} = 0.12$ and $\beta_{\text{scat}} = 0.173$. The implied mass of each jet is changed from the $0.1 M_{\odot}$ to $0.4 M_{\odot}$: this follows from holding the ratio M/β_{in}^2 fixed in equation (7) (see § 2) so that the other values in that equation can stay unchanged. This mass is a relatively large fraction of a typical SN Ib where total ejecta mass is perhaps only $4 M_{\odot}$ or less (e.g., Hachisu et al. 1991).

In the Figure 6 calculation, the wavelength of jet-scattered flux is increased by a factor of 1.173 (see § 3.3, eq. [29] with $\mu = 0$) which is so large that the jet-scattered flux comes from direct flux spectrum wavelength regions where the continuum levels can be rather different than those of the wavelength regions to which the scattered flux is added to give the net spectrum. A result of this large redshift is that polarization at the blue end of the optical is somewhat reduced in overall continuum trend relative the Figure 5 case. The polarized flux in the blue part originates in even bluer flux of the direct spectrum: but since the direct spectrum declines blueward on average, there is less polarized flux at a given wavelength than if the redshift were smaller.

Figure 6 like Figure 5 shows inverted P Cygni polarization profiles.

5. Conclusions and Final Discussion

We have proposed a bipolar jet model for supernova polarization. The motivation for this model is to resolve the potential paradox set by BBK analysis which suggests strong spherical symmetry for Type Ib supernovae (see § 1.2) and the expectation that Type Ib supernovae should be highly polarized in the continuum up to perhaps $\sim 4\%$ (see § 1.1). For the model, we have derived simple, non-relativistic approximate analytic formulae for relative scattered flux R (i.e., for the ratio of scattered flux to direct flux from the bulk supernova) and for polarization (see eq. [47] and [48] of § 3.5). The polarization formula qualitatively reproduces two main features observed for at least some supernovae: (1) the rise of continuum polarization to a maximum and then a decline with time (see § 4.2); (2) the inverted P Cygni polarization profiles of lines (see § 4.4). The level of continuum and line polarization obtained reaches that observed for supernovae (i.e., of order a percent or a few percent: see § 1.1) for plausible jet model parameters: in fact, one set of plausible parameters does allow continuum polarization to reach $\sim 4\%$ (see § 4.2). The position of angle polarization is a constant for the bipolar jet model since it is a strictly axisymmetric model and the model does not allow 90° shifts in position angle which are possible for axisymmetric models in general. Since position angle variation is observed, the model cannot account for all the polarization of all supernovae.

The bipolar jet model predicts that two kinds of the polarization plateau phases in time can exist (see § 2). The first kind of plateau phase is unavoidable and should be observable if a supernova with jets (of the kind we have posited) is observed early enough: we show cases of this plateau phase in Figures 1, 2, and 3 in § 4.2. The second kind can only exist if $b \gg 2$ (see § 2): we show cases with and without the second kind of plateau phase in Figures 1, 2 and 3 in § 4.2. The second kind is probably physically unrealizable for jets wide enough to give observationally significant continuum polarization (see § 4.2). We have not yet examined existing supernova polarization data to find evidence for the kinds of polarization plateaus predicted by the bipolar jet model.

We derived the analytic formulae for relative scattered flux and polarization using very simplifying assumptions. We have treated the electron optical depth structure of the jets very crudely and neglected any line or other opacity in them. The geometry of the supernova-jet structure has also been treated crudely (see § 2). The time-delay effect (see § 3.2) can be included in the model, but it can be neglected for simplicity as we have done in deriving the analytic formulae and in the demonstration calculations. We have assumed the bulk

supernova (i.e., the supernova not counting the jets) is spherically symmetric: this cannot be completely true although to resolve the potential paradox it must be roughly true.

There are 5 independent basic parameters for the bipolar jet model: θ (or $\mu = \cos \theta$), $\Delta\theta$, τ_{rad} , β_{in} , and b (see § 3.5) which unfortunately are rather degenerate particularly for the analysis of a single polarization epoch. For an analysis of the time evolution of the polarization the $\tau_{\text{rad}} t_0^2$ parameter (see § 2, esp. eq. [9]) can replace τ_{rad} as one of the 5 independent basic parameters. In an analysis in which the time-delay effect is included, t_{red} (see § 3.2) replaces τ_{rad} as one of the 5 independent basic parameters.

We have neglected relativistic effects in our formalism. If β_{scat} becomes sufficiently large (e.g., $\gtrsim 0.1$), then this neglect could be a significant limitation of the formalism since relativistic effects will be important. These effects could significantly reduce the calculated supernova polarization relative cases that neglect them, but have otherwise the same parameters. The essential reason is that energy is lost from scattered flux by Doppler shifting into the jet frame that is not regained Doppler shifting back to the rest frame of the supernova center. If the jet-scattered flux decreases because of this process, then the amount of polarized flux decreases and net polarization decreases. Thus, our formulation may overestimate polarization for jets that are too relativistic. In future work we intend to investigate relativistic effects in the bipolar jet model.

Because of our simplifying assumptions, the derived formulae can only be expected to semi-quantitatively reproduce the effects of bipolar jets and, of course, the parameters used in the formulae will have only a crude relation to the parameters of actual bipolar jets which we expect to have rather complex structure. The formulae should be tested by Monte Carlo calculations. Such tests would probably show how to adjust the formulae to improve their quantitative accuracy. In any case, variations on the formulae we have presented are clearly possible. In the analysis of actual supernova polarimetric data, some variations may turn out to be obviously more appropriate than formulae we have given.

The advantage of the analytic formulae is that they allow a straightforward, intelligible analysis of polarimetry data by fitting the data and they allow a simple first-order approach to testing the adequacy of the bipolar jet model. We have verified the adequacy of the model to some degree in this paper: see the first paragraph of this section. If the model’s adequacy is further verified, then more a more elaborate testing procedure for the model should be considered. For example the calculation of polarization spectra using Monte Carlo radiative transfer for a bipolar jet model whose structure is produced—if it is feasible—by a realistic hydrodynamic calculation.

In this paper, we have only considered the bipolar jet model with SNe Ib in mind. The

bipolar jet model may apply generally to core-collapse supernovae. On the other hand it may only to apply to some: i.e., some SNe Ib and, perhaps, some of their smaller-envelope kin, Type Ic supernovae. In future work we hope to test the bipolar jet model using polarimetry and spectropolarimetry from all types of core-collapse supernovae.

As final word, one must emphasize that neither the bipolar jet model nor the other models of supernova asymmetry (see § 1.1) are exclusive. Several kinds of asymmetry can be present for a single supernova. For example, Type Ic supernova SN 2002ap shows a component of polarization that can modeled by a jet (Kawabata et al. 2002; Leonard et al. 2002). There is certainly another polarization component present though in SN 2002ap perhaps due to a inner ejecta asymmetry of order 10 % in axis ratio projected on the sky (Kawabata et al. 2002; Wang et al. 2003). The late direct HST imaging of SN 1987A confirms that in one supernova at least, there is a large inner ejecta asymmetry: the major to minor axis ratio of images is of order 1.5/1 (Wang et al. 2002). It may be that such inner ejecta asymmetry (caused perhaps by non-relativistic, never-emergent bipolar jets: Höflich et al. 2001) is the main kind of SN 1987A asymmetry. However, a re-analysis of early SN 1987A speckle interferometry (Nisenson & Papaliolios 1999) suggests that relativistic jets (with perhaps $\beta \sim 0.8$) did emerge from SN 1987A in addition to other asymmetries. These suggested jets, however, may have been too relativistic to have contributed significantly to SN 1987A’s polarization: this a subject for further study.

I thank David Branch and Eddie Baron for stimulating this work and their comments on it. Support for the paper was provided by the Departments of Physics of New Mexico Tech and the University of Nevada, Las Vegas, and the Department of Physics and Astronomy of the University of Oklahoma. This research has made use of the NASA/IPAC Extragalactic Database (NED) which is operated by the Jet Propulsion Laboratory, California Institute of Technology, under contract with the National Aeronautics and Space Administration.

REFERENCES

- Baron, E. 2001, private communication
- Branch, D., et al. 2002, ApJ, 566, 1005, astro-ph/0106367 (BBK)
- Cappellaro, E., & Turatto, M. 2001, in The Influence of Binaries on Stellar Population Studies, Astrophysics and space science library (ASSL), Vol. 264, ed. D. Vanbeveren, (Dordrecht: Kluwer Academic), 199, astro-ph/0012455
- Cardelli, J. A., Clayton, G. C., & Mathis, J. S. 1989, ApJ, 345, 245.

- Cassinelli, J. P., & Hummer, D. G. 1971, MNRAS, 154, 9
- Chandrasekhar, S. 1960, Radiative Transfer (New York: Dover Publications, Inc.)
- Chugai, N. N. 1992, Sov. Astron. Lett., 18(3), 168
- Clayton, D. D. 1983, Principles of Stellar Evolution and Nucleosynthesis (Chicago: University of Chicago Press)
- Clocchiatti, A., Wheeler, J. C., Brotherton, M. S., Cochran, A. L., Wills, D., Barker, E. S., & Turatto, M. 1996, ApJ, 462, 462
- Davisson, C. M. 1965, in Alpha-, Beta-, and Gamma-Ray Spectroscopy, ed. K. Siegbahn (Amsterdam: North-Holland Publishing Company), 37
- Filippenko, A. V. 1997, ARA&A, 35, 309
- Filippenko, A. V., et al. 1995, ApJ, 450, L11
- Hachisu, I., Matsuda, T., Nomoto, K., & Shigeyama, T. 1991, ApJ, 368, L27
- Harkness, R. P. 1991, in ESO/EIPC Workshop: SN 1987A and Other Supernovae, ed. I. J. Danziger & K. Kj  r (Garching: ESO), 447
- H  flich, P. 1991, A&A, 246, 481
- H  flich, P., Khokhlov, A., & Wang, L. 2001, in 20th Texas Symposium on Relativistic Astrophysics, ed. J. C. Wheeler & H. Martel (Melville, New York: American Institute of Physics), 459, astro-ph/0104025
- Howell, D. A., H  flich, P., Wang, L., & Wheeler, J. C. 2001, ApJ, 556, 302, astro-ph/0101520
- Janka, H.-Th., Buras, R., Kitaura Joyanes, F. S., Marek, A., & Rampp, M. 2004, in Procs. 12th Workshop on Nuclear Astrophysics, Ringberg Castle, in press, astro-ph/0405289
- Jeffery, D. J. 1989, ApJS, 71, 951
- Jeffery, D. J. 1991a, ApJ, 375, 264
- Jeffery, D. J. 1991b, ApJS, 77, 405
- Jeffery, D.J. 1999, astro-ph/9907015
- Kawabata, K. S. 2002, ApJL, 580, L39, astro-ph/0205414

- Leonard, D. C., & Filippenko, A. V. 2001, PASP, 113, 920 astro-ph/0105295
- Leonard, D. C., Filippenko, A. V., Ardila, D. R., & Brotherton, M. S. 2001, ApJ, 553, 861, astro-ph/0009285
- Leonard, D. C., Filippenko, A. V., Barth, A. J., & Matheson, T. 2000a, ApJ, 536, 239, astro-ph/9908040
- Leonard, D. C., Filippenko, A. V., Chornock, R., & Foley, R. J. 2002, PASP, 114, 1333, astro-ph/0206368
- Leonard, D. C., Filippenko, & Matheson, T. 2000b in Cosmic Explosions, ed. S. S. Holt & W. W. Zhang (New York: AIP), 165
- MacFadyen, A. I., Woosley, S. E., & Heger, A. 2001, ApJ, 550, 410
- Matheson, T., Filippenko, A. V., Li, W., Leonard, D. C., & Shields, J. C. 2001, AJ, 121, 1648
- McCall, M. L. 1984, MNRAS, 210, 829
- McCall, M. L. 1985, in Supernovae as Distance Indicators, ed. N. Bartel (Berlin: Springer-Verlag), 48.
- McCall, M. L. 2001, private communication
- Méndez, M. 1990, private communication
- Mihalas, D. 1978, Stellar Atmospheres, (San Francisco: W. H. Freeman and Company)
- Nisenson, P., & Papaliolios, C. 1999, ApJ, 518, L29, astro-ph/9904109
- O'Donnell, J. E. 1994, ApJ, 422, 158.
- Serkowski, K. 1973, in IAU Symposium 52, Interstellar Dust and Related Topics, ed. J. M. Greenberg & H. C. van de Hulst (Dordrecht: Reidel), 145
- Shapiro, P. R., & Sutherland, P. G. 1982, ApJ, 263, 902
- Shigeyama, T., Suzuki, T., Kumagai, S., Nomoto, K., Saio, H., & Yamaoka, H. 1994, ApJ, 420, 341
- Wagoner, R. V. 1981, ApJ, 250, L65
- Wang, L., Baade, D., & Höflich, P., & Wheeler, J. C., 2003, ApJ, 592, 457, astro-ph/0206386

- Wang, L., Howell, D. A., Höflich, P., & Wheeler, J. C. 2001, ApJ, 550, 1030, astro-ph/9912033
- Wang, L., & Wheeler, J. C. 1996, ApJ, 462, L27
- Wang, L., Wheeler, J. C., & Höflich, P. 1997, ApJ, 476, L27
- Wang, L., et al. 2002, ApJ, 579, 677, astro-ph/0205337
- Wang, L., Wheeler, J. C., Li, Z.-W., & Clocchiatti, A. 1996, ApJ, 467, 435, astro-ph/9602155
- Wheeler, J. C., & Benetti, S. 2000, in Allen’s Astrophysical Quantities, 4th Edition, ed. A. N. Cox (New York: Springer-Verlag; AIP), 451
- Woosley, S. E., & Weaver, T. A. 1994, in Supernovae: Session LIV of the Les Houches École d’Été de Physique Théorique, ed. S. A. Bludman, R. Mochkovitch, & J. Zinn-Justin (Amsterdam: North-Holland), 63
- Zhang, W., Woosley, S. E., & MacFadyen, A. I. 2003, ApJ, 586, 356, astro-ph/0207436

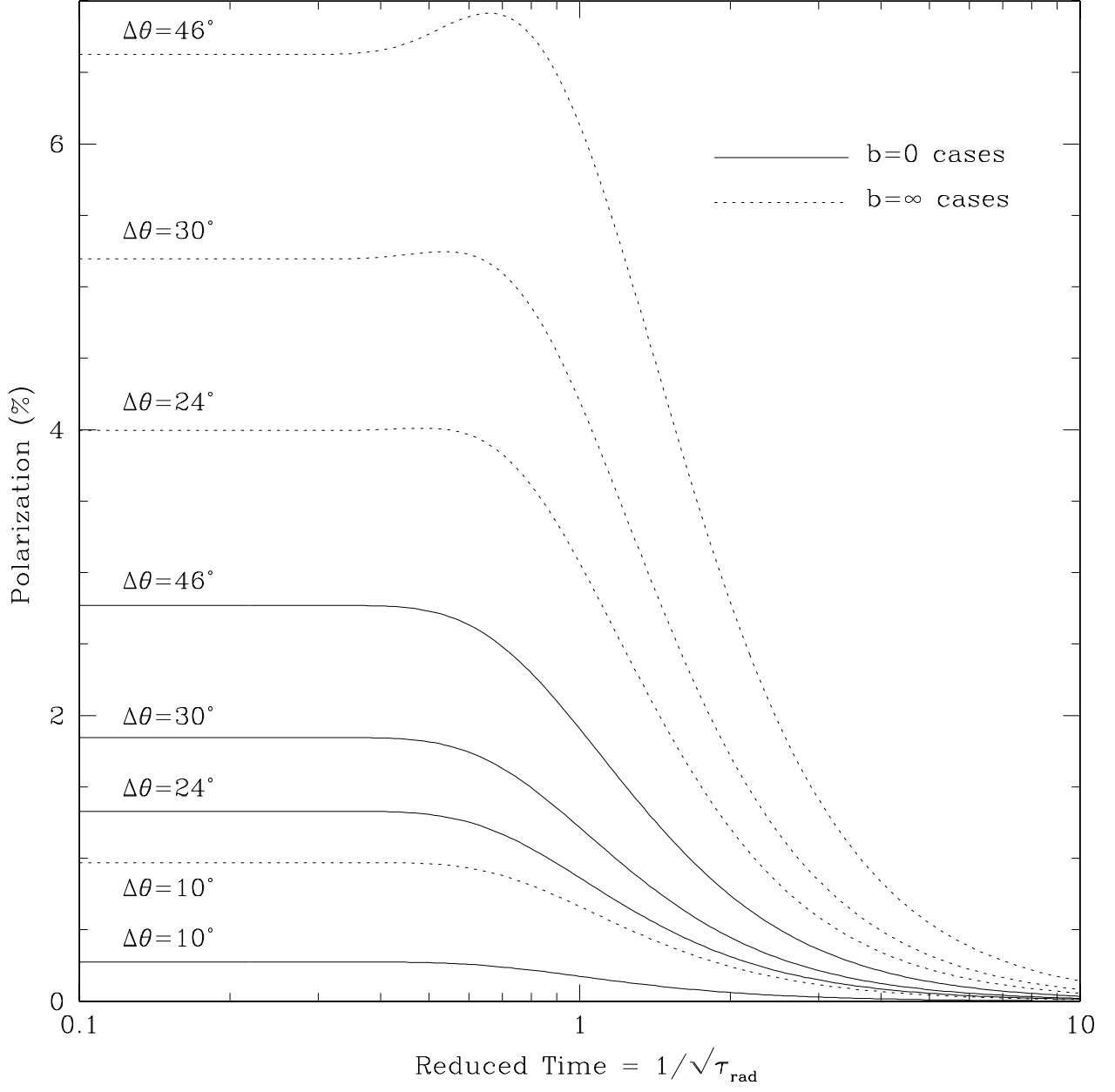


Fig. 1.— Continuum polarization as a function of reduced time for a range of $\Delta\theta$ values as specified on the figure, and $b = 0$ and $b = \infty$. We have set $\theta = 90^\circ$ and the direct supernova flux is wavelength independent. The later condition means that $[f_{\text{dir}}(\lambda'_+)(1 - \omega_\mu\mu) + f_{\text{dir}}(\lambda'_-)(1 + \omega_\mu\mu)]/f_{\text{dir}}(\lambda) = 2$, and the β_{in} parameter is not used and is left unspecified.

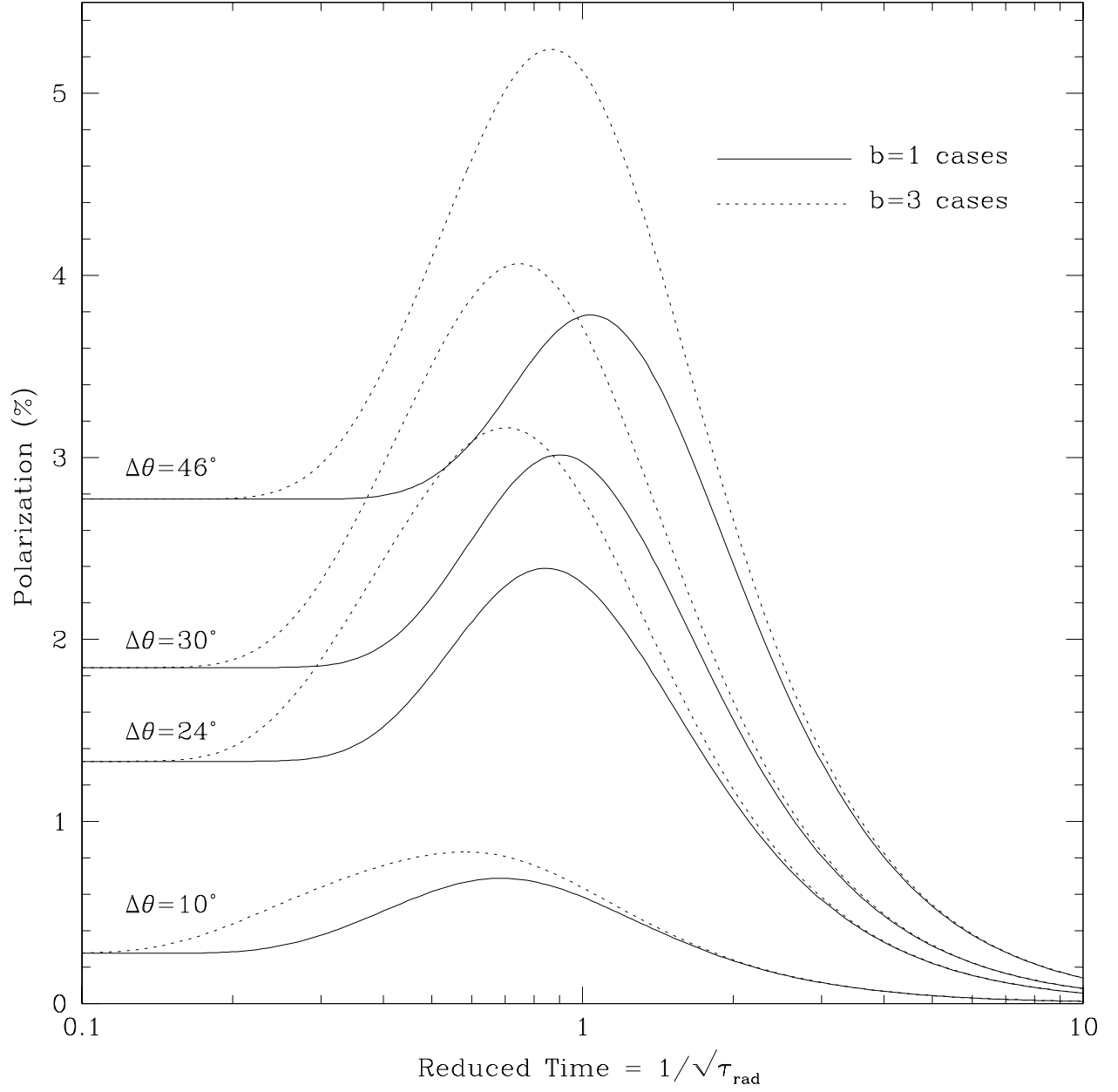


Fig. 2.— The same as Figure 1, except the polarization curves are for $b = 1$ and $b = 3$.

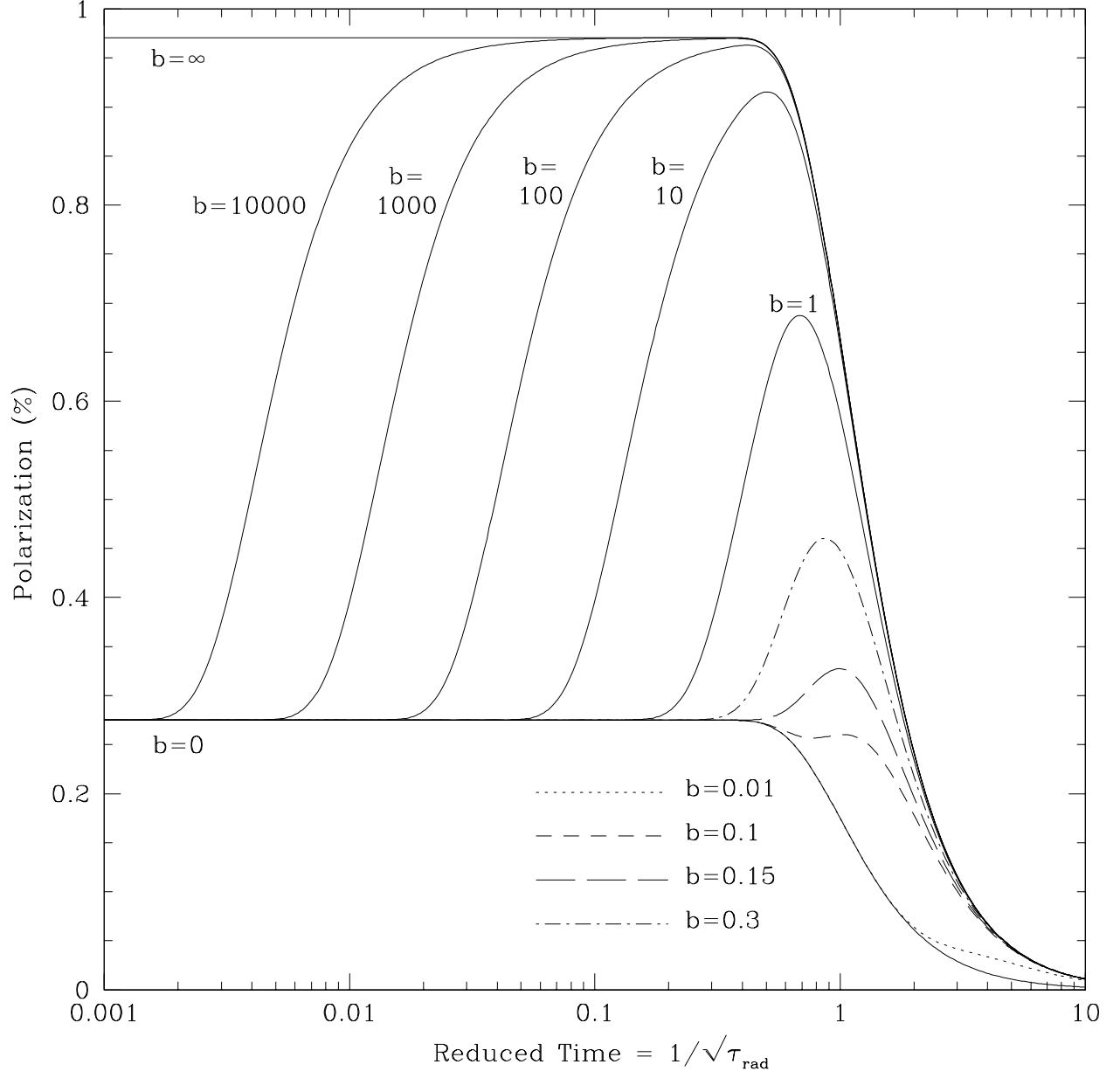


Fig. 3.— The same as Figure 1, except that $\Delta\theta$ is set to 10° and a range of b values as specified on the figure are used.

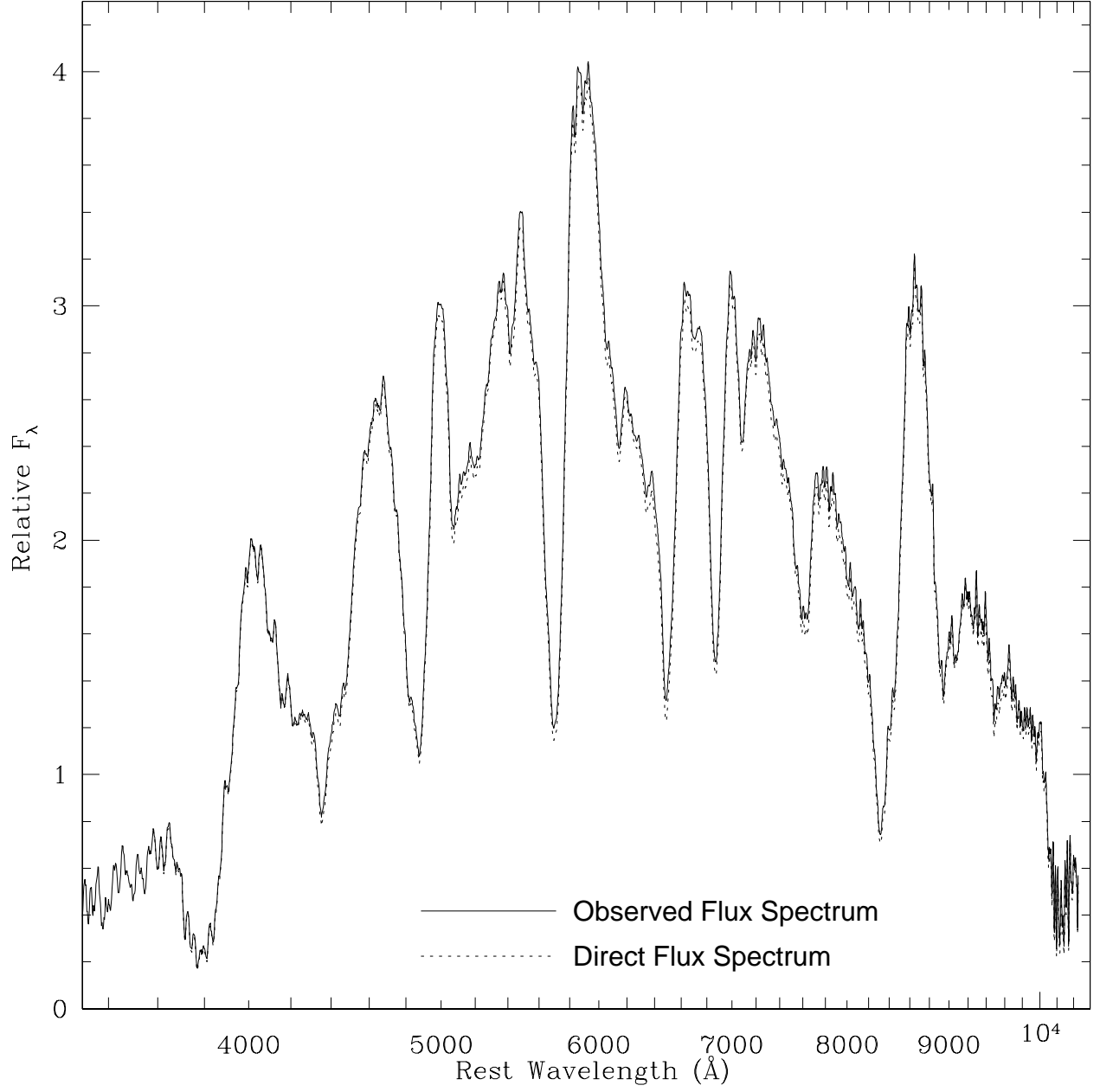


Fig. 4.— The observed flux spectrum and bipolar jet model direct flux spectrum of SN 1999dn for day 17 past V maximum. The scale of the spectra is arbitrary. The bipolar jet model parameters are specified in the text (see § 4.4). Both spectra have been corrected for heliocentric velocity redshift and foreground Galactic extinction.

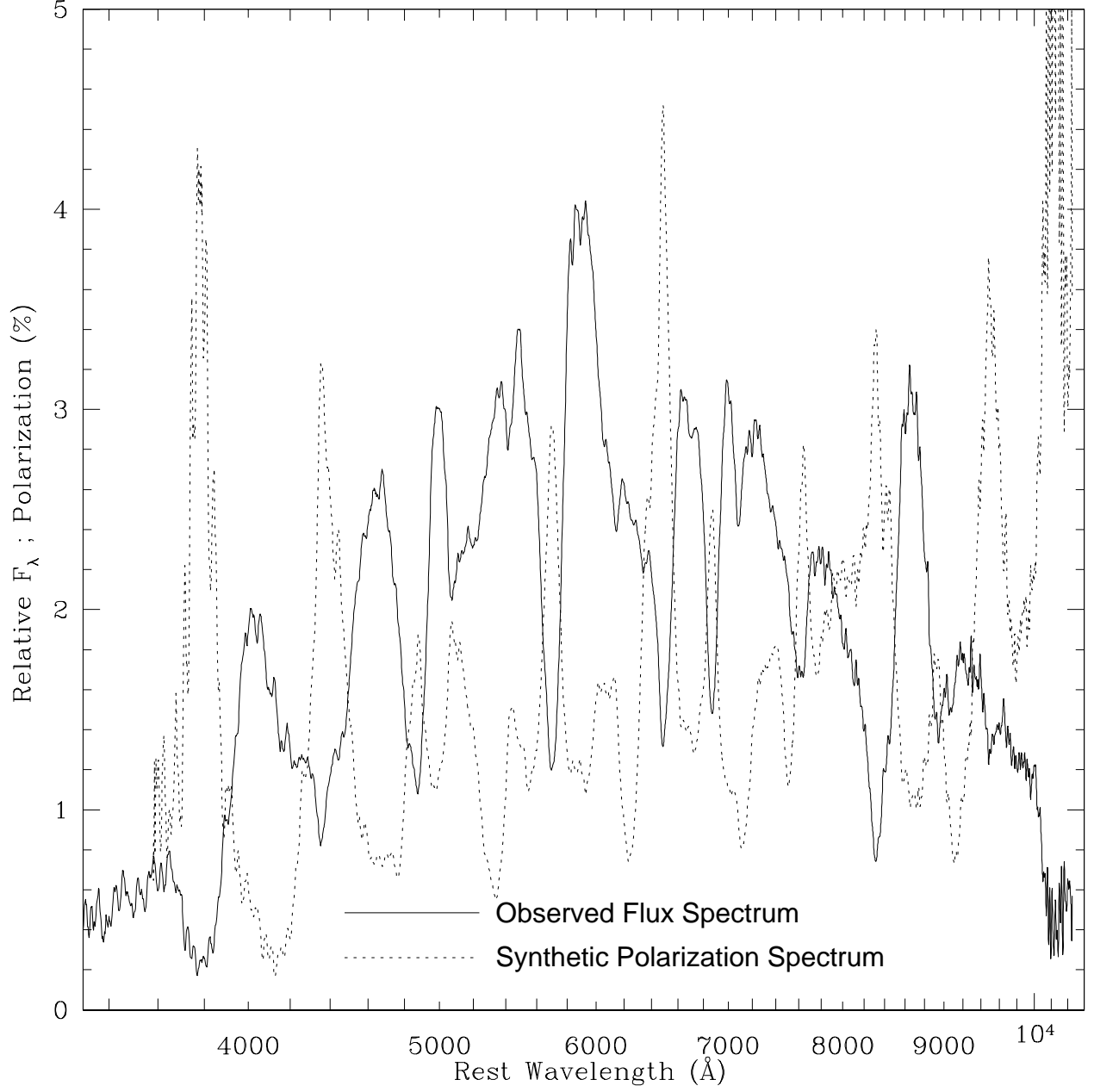


Fig. 5.— The bipolar jet model polarization spectrum for the observed flux spectrum of Fig. 4 which is shown overlaid. The bipolar jet model parameters are the same as for Fig. 4 and are specified in the text (see § 4.4).

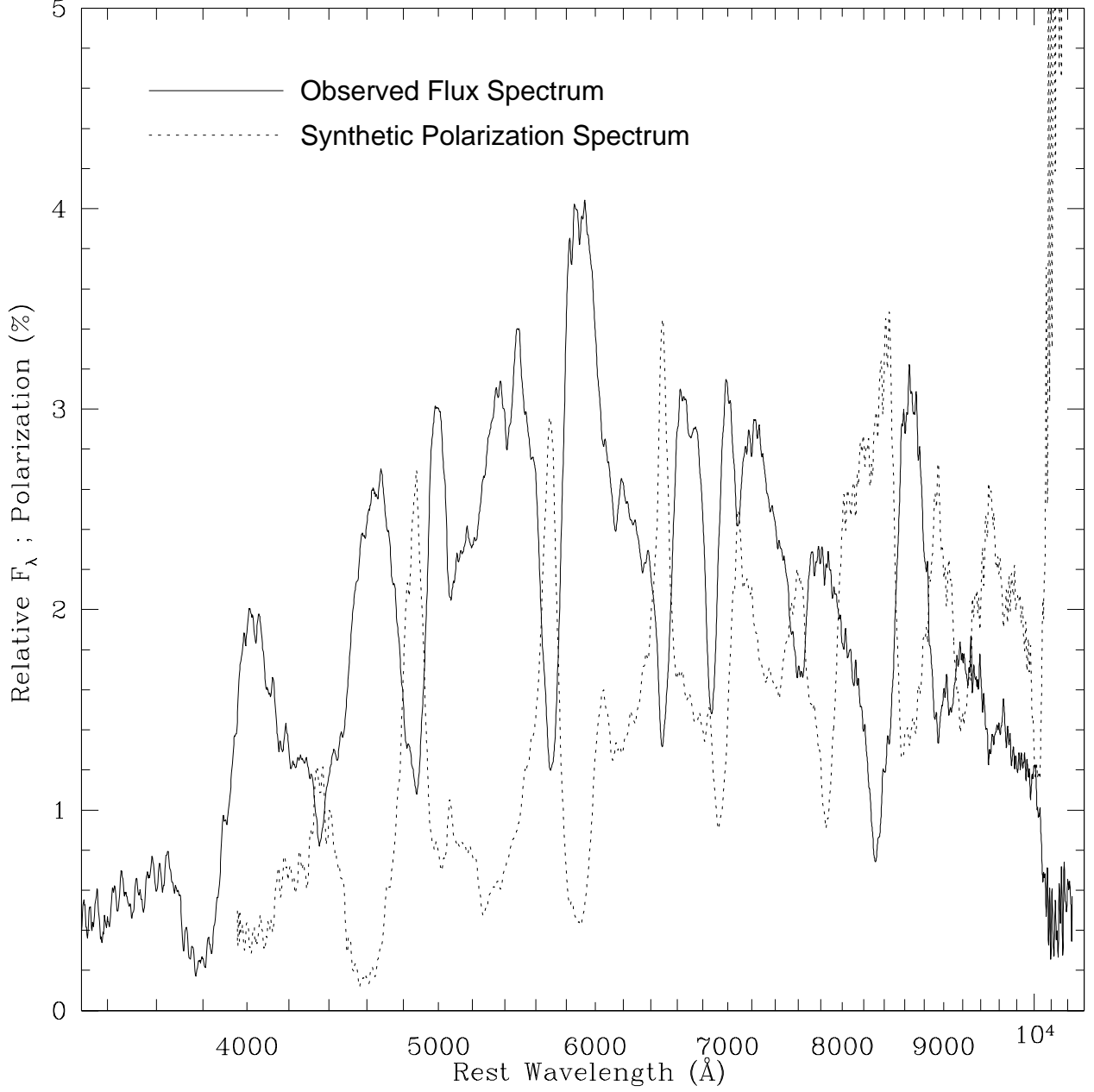


Fig. 6.— The bipolar jet model polarization spectrum for the observed flux spectrum of Fig. 4 which is shown overlaid. The bipolar jet model parameters are as for Figs. 4 and 5 (see text § 4.4), except the β_{in} parameter has been doubled from 0.06 to 0.12. This greatly increases the redshift effect of the jets.

Table 1. Runs of High Continuum Polarization and Ancillary Quantities as Functions $\Delta\theta$ for the Radial Phase of the Bipolar Jet Model

$\Delta\theta$ ($^\circ$)	$\Omega_{\text{fr}}(\Delta\theta)$	$\xi(\Delta\theta)$	w	R	P (%)
0	0	1	1	0	0
1	7.6×10^{-5}	0.9998	0.9870	1.1×10^{-4}	0.0113
3	6.9×10^{-4}	0.9982	0.9617	0.0010	0.0986
7	0.0037	0.9901	0.9137	0.0058	0.5029
10	0.0076	0.9798	0.8799	0.0119	0.9708
15	0.0170	0.9549	0.8272	0.0270	1.9657
20	0.0302	0.9207	0.7790	0.0486	3.0939
24	0.0432	0.8871	0.7433	0.0704	3.9944
30	0.0670	0.8270	0.6943	0.1107	5.1942
40	0.1170	0.7053	0.6231	0.1975	6.4399
46	0.1527	0.6224	0.5860	0.2606	6.6262 ^a
50	0.1786	0.5643	0.5634	0.3069	6.5166
60	0.2500	0.4135	0.5132	0.4359	5.5421

^aMaximum continuum polarization (for the chosen parameters) as a function of $\Delta\theta$. To better numerical accuracy it is 6.6271108 % at 45.600748 $^\circ$.

Note. — The predictions were calculated using equation (47) for R and equation (48) for P assuming a wavelength independent direct flux from the bulk supernova. The fixed parameter values for the predictions are $\theta = 90^\circ$, $b = \infty$, and $\tau_{\text{rad}} \gg 1$ (see text, § 4.1). The β_{in} parameter is not specified since it is irrelevant to the calculation.